Climatic cycles inferred from the aminostratigraphy and aminochronology of Quaternary dunes and palaeosols from the eastern islands of the Canary Archipelago

J. E. ORTIZ,[1]* T. TORRES,[1] Y. YANES,[2] C. CASTILLO,[2] J. DE LA NUEZ,[3] M. IBÁÑEZ[2] and M. R. ALONSO[2]
[1] Laboratorio de Estratigrafía Biomolecular, Escuela Técnica Superior de Ingenieros de Minas de Madrid, Madrid, Spain
[2] Departamento de Biología Animal, Facultad de Biología, Universidad de La Laguna, La Laguna, Tenerife, Canary Islands, Spain
[3] Departamento de Edafología y Geología, Facultad de Biología, Universidad de La Laguna, La Laguna, Tenerife, Canary Islands, Spain

ABSTRACT: Aminochronological and aminostratigraphical methods have been used to study the Quaternary aeolian deposits from the islands located east of the Canary Archipelago (Fuerteventura and Lanzarote islands and La Graciosa, Montaña Clara and Alegranza islets). The extent of racemisation/epimerisation of four amino acids (isoleucine, aspartic acid, phenylalanine and glutamic acid) was measured in land snail shells of the genus *Theba*. The age calculation algorithms of these amino acids have been determined to permit the numerical dating of these deposits. Eight Aminozones, each defining dune/palaeosol-formation episodes, have been distinguished and dated at 48.6 ± 6.4, 42.5 ± 6.0, 37.8 ± 4.6, 29.4 ± 4.8, 22.4 ± 4.5, 14.9 ± 3.6, 11.0 ± 4.0 and 5.4 ± 1.1 ka BP, the first five of them defining cycles of 5–7 ka.

The alternation of palaeosols and aeolian deposits, which are related to abrupt transitions from humid to arid conditions, are the reflection of globally induced changes in North Africa palaeoenvironmental conditions linked to the effect of African palaeomonsoons on the trade winds and the Saharan Air Layer. Probably these aeolian cycles, with a recurrence period of 5–7 ka, are the expression of multiples of the ~2.4 ka solar-cycle

Introduction

Fuerteventura and Lanzarote islands and La Graciosa, Montaña Clara and Alegranza islets (north of Lanzarote Island) are located in the east part of the Canary Archipelago (Fig. 1), about 100 km off the coast of Africa. They are characterised by an arid climate (annual rainfall is ca. 100 mm) and they are considered to be the western outpost of the Saharan Zone. This Archipelago is located in a region of strong interaction between atmospheric and ocean circulation systems. The major source of terrigenous sediments is the trade winds, which drive seasonal coastal upwelling, and the dust storms from the neighbouring Sahara Desert.

These islands and islets are composed of a variety of mostly volcanic rocks. Likewise, Quaternary palaeosols interbedded with aeolian deposits (dunes) occur (Fig. 2), providing palaeoclimatic information, i.e. they represent the alternation of humid and arid episodes (Petit-Maire *et al.*, 1986, 1987; Rognon and Coudé-Gaussen, 1988, 1996a; Damnati *et al.*, 1996; Damnati, 1997; Castillo *et al.*, 2002).

According to Damnati *et al.* (1996) and Damnati (1997), the aeolian deposits consist mainly of carbonate sands, while the palaeosols are dominated by lutites. The clay mineralogy suggests an allochthonous origin to that part of the sediments related to dust transport from the western Sahara Desert. Previous studies have shown that some of the aeolian deposits from Fuerteventura and Lanzarote Islands have been accumulated during MIS 1 and 3 (Petit-Maire *et al.*, 1986; Hillaire-Marcel *et al.*, 1995; Damnati *et al.*, 1996; De La Nuez *et al.*, 1997; Meco *et al.*, 1997). These dune-formations contain abundant remains of land snails (Fig. 2) and vertebrates, some of them extinct (Michaux *et al.*, 1991; Boye *et al.*, 1992; Castillo *et al.*, 1996), as well as abundant ichnofossils (Fig. 2), mainly produced by hymenopters (Ellis and Ellis-Adam, 1993; Edwards and Meco, 2000; Alonso-Zarza and

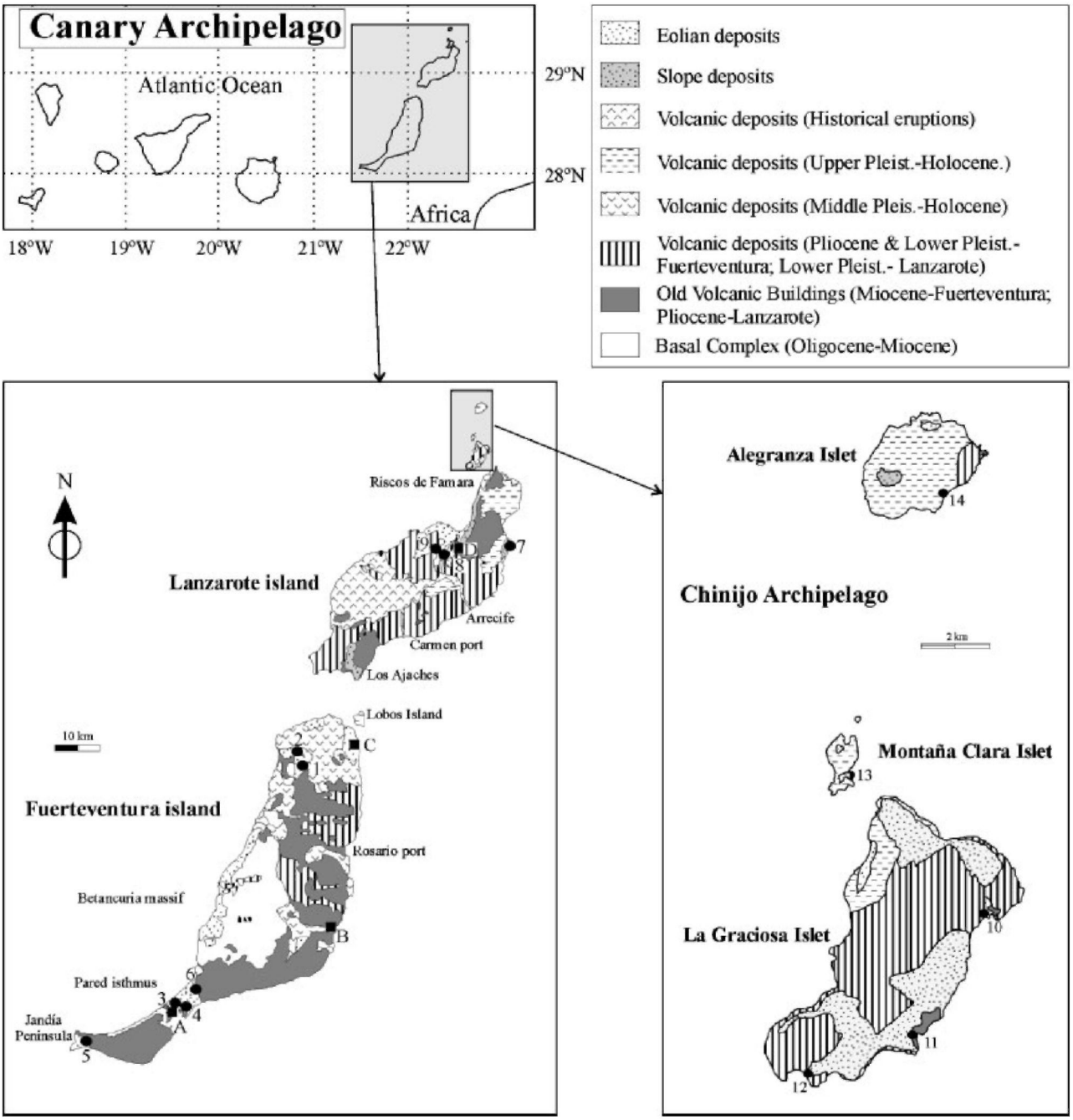

Figure 1 Geographical location and geology of Fuerteventura and Lanzarote islands and La Graciosa, Montaña Clara and Alegranza islets with the situation of the stratigraphic sections in circles (modified from Ancochea *et al.*, 1996; 2004): (1) Barranco de los Encantados (FBE), (2) Montaña de la Costilla (FMC), (3) Barranco del Pecenescal (FBP), (4) Atalayeja Grande (FAG), (5) Montaña Azufrá (FMA), (6) Hueso del Caballo (FHC), (7) Mala (LMA), (8) Loma de San Andrés (LLA), (9) Tao (LTA), (10) Morros Negros (GMN), (11) Caleta del Sebo (GCS), (12) La Cocina (GLC), (13) Caleta de Guzmán (MCG), (14) Montaña Lobos (AML). Other sections cited in the text are also indicated in the figure (in squares): Jandía (A), Pozo Negro (B), Corralejo (C), Teguise (D). Rosa Negra section is also called Montaña de la Costilla (2)

Silva, 2002) and coleopters (Genise and Edwards, 2003). High degrees of species diversity and endemicity (Yanes *et al.*, 2004) characterise the land snail assemblages. However, geochronological studies of these deposits are scarce and unconnected.

Among the different dating methods applied, amino acid racemisation has become increasingly common. The method is based on the fact that living organisms contain only L-amino acids which gradually racemise (epimerise) into D-amino acids after death. Thus, the D/L ratio increases with time after death until it is equal to 1 (1.3 for isoleucine), that is, when equilibrium is reached. The racemisation/epimerisation process is a first-order-reversible chemical reaction, which is genus- and temperature-dependent.

Amino acid racemisation dating has been successfully used for the correlation and dating of aeolianites from different areas around the world, such as Madeira (Goodfriend *et al.*, 1996), Bahamas (Kindler and Hearty, 1995; Hearty *et al.*, 1999), Bermuda (Vacher *et al.*, 1995), islands close to Australia (Murray-Wallace *et al.*, 2001, Brooke *et al.*, 2003; Hearty, 2003) and the Hawaiian islands (Hearty *et al.*, 2000). This method offers several advantages compared to other dating methods: only a small sample is necessary for a single analysis (20–60 mg), different kinds of samples are suitable, including

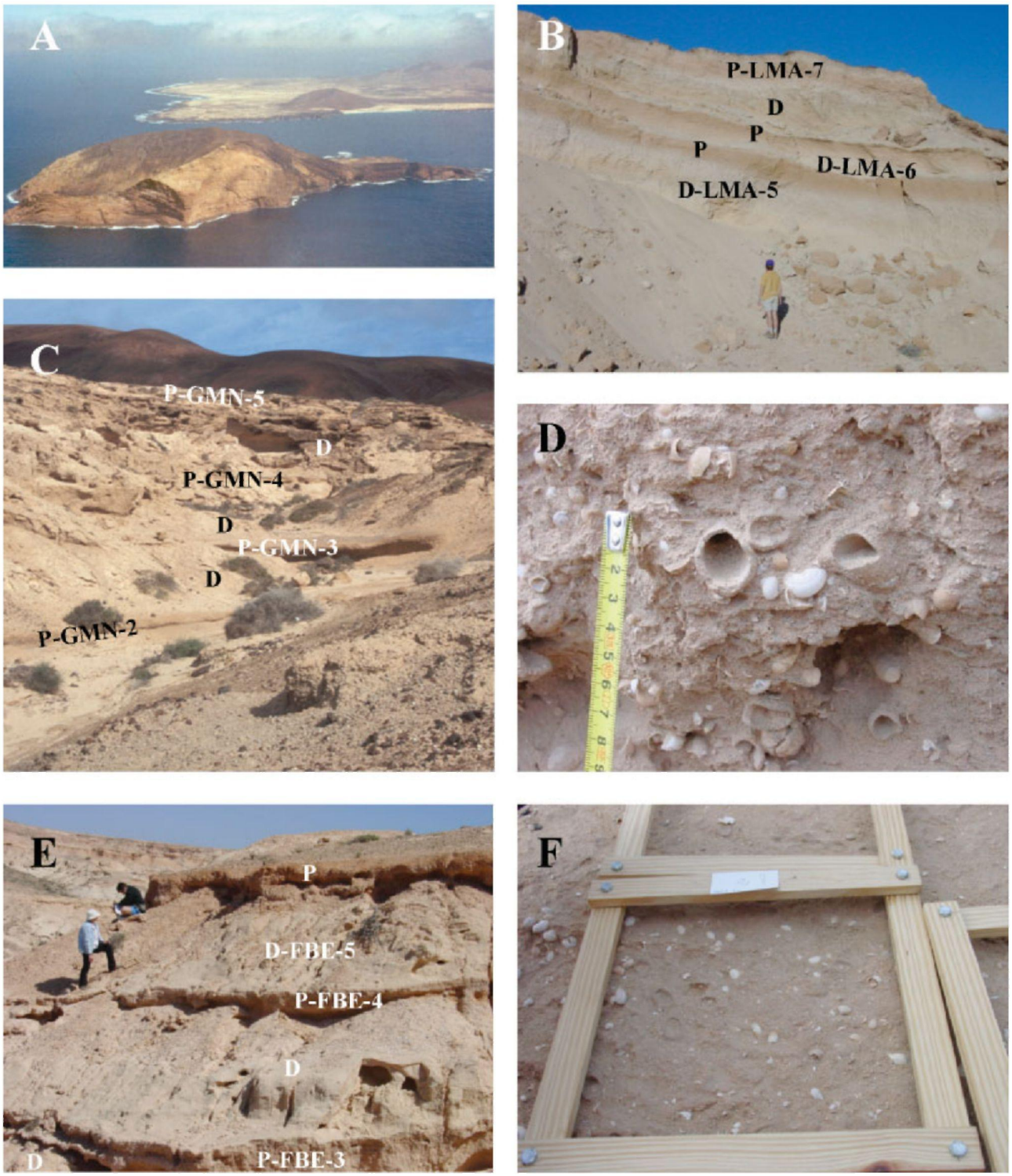

Figure 2 Photographs of the Canary Islands aeolian/palaeosol sequences. A: aerial view of Montaña Clara (front) and La Graciosa (rear) islets, composed of volcanic rocks. B: Upper part of the Mala stratigraphic section, Lanzarote Island (LMA), where palaeosols (P) interbedded with aeolian deposits (dunes-D) appear. C: Lower part of Morros Negros stratigraphic section, with palaeosols (P) and dune deposits (D). D: Land snail shells and insect nests from bed GCS-1 (the scale is in cm). E: Middle part of Barranco de los Encantados section, Fuerteventura Island (FBE), with aeolian deposits (D) and palaeosols (P). F: Lag deposit of land snail shells, consisting mostly in *Theba geminata*, from bed GCS-2 (grid size is 1 m^2). Sampled horizons are marked in the photographs

mollusc shells, and the method can be used beyond the range of radiocarbon and partially beyond that of U/Th. Gastropod shells are particularly useful for amino acid racemisation/epimerisation dating, as their non-porous shell structure minimises contamination (Hare and Mitterer, 1968). Thus, it has been successfully used for the dating of gastropod shells (Goodfriend, 1987a, 1991, 1992; Goodfriend and Mitterer, 1988; Meyer, 1992; Torres *et al.*, 1997; Ortiz *et al.*, 2002; Brooke *et al.*, 2003).

The aim of this paper is to define, correlate and date the different aeolian episodes built up on the Fuerteventura and Lanzarote islands and La Graciosa, Montaña Clara and Alegranza islets through amino acid racemisation analysis of fossil land snails. We have selected shells belonging to the genus *Theba*. Because the amino acid racemisation is not a numerical dating method in isolation, it needs to be calibrated, mainly by radiometric dating methods. In this paper, the age

calculation algorithms for four amino acids (isoleucine, aspartic acid, phenylalanine and glutamic acid) will be established using samples previously dated by radiocarbon (De La Nuez *et al.*, 1997) as well as new datings shown in this paper. Our results will be compared with others previously published in order to establish the stratigraphical framework of these aeolian deposits. Finally, their palaeoclimatic significance will be discussed.

Geographical location and geological context

Fuerteventura and Lanzarote islands and the Chinijo Archipelago (La Graciosa, Montaña Clara and Alegranza islets) are the easternmost islands of the Canary Archipelago. They consist of volcanic rocks erupted in three main cycles (Coello *et al.*, 1992): the first one was of submarine character with hyperabyssal roots (plutons and dykes) with successive subaerial growth (Ancochea *et al.*, 1996), and is called the 'Basal Complex' accumulation; the second one produced subaerial flows during the Miocene (20–12 Ma), although volcanic activity prevailed in Lanzarote Island until 5 Ma; and finally, after a period of volcanic inactivity and erosion, another episode of subaerial eruptions (more limited than the previous one) took place (Pliocene–Pleistocene–Holocene). These islands and islets form part of the same insular shelf.

An important geomorphological feature is the development of 'jable' (in local terminology), which consists of aeolian deposits made of marine-origin bioclastic sand, in some cases covering wide areas, such as on Fuerteventura Island and La Graciosa Islet (Fig. 1). Many stratigraphic sections have been studied and sampled (Fig. 1; Table 1). Each section was named using three letters according to the island/islet on which it is located and the initial letters of the section, e.g. Morros Negros (La Graciosa Islet) is named GMN.

Fuerteventura Island is 1662 km^2, with its major peak (Zarza peak) reaching 807 m a.s.l. It is the oldest island of the Canary Archipelago and one of the few where the 'Basal Complex' materials crop out (Coello *et al.*, 1992; Ancochea *et al.*, 1996). Volcanic rocks erupted during the Miocene together with basalts dated at Pliocene, Pleistocene and Holocene also appear. Six stratigraphic aeolian sections have been studied and sampled (Figs 1 and 3; Table 1): Barranco de los Encantados (FBE), Montaña de la Costilla (FMC), Barranco del Pecenescal (FBP), Atalayeja Grande (FAG), Montaña Azufrá (FMA), and Hueso del Caballo (FHC).

Lanzarote Island is the second oldest island of the Canary Archipelago, with an area of 833 km^2 and a highest elevation of 670 m a.s.l. (Riscos de Famara). Miocene to Holocene age volcanic materials are commonly found here (Carracedo and Rodríguez, 1993; Coello *et al.*, 1992). Aeolian deposits are observed only across the north part of the island and have been studied (Figs 1 and 4; Table 1): Mala (LMA), Loma de San Andrés (LLA) and Tao (LTA).

The Chinijo Archipelago is located north of Lanzarote Island and comprises La Graciosa, Montaña Clara and Alegranza islets (Fig. 1). These islets are composed of Lower Pleistocene and Upper Pleistocene–Holocene volcanic sequences, made of cinder cones and hydromagmatic centres on a flat platform (Fúster *et al.*, 1968; Quesada *et al.*, 1992). La Graciosa is the biggest islet (27 km^2) where the oldest volcanic rocks appear below more than 1 m of fossil beach (Series III of Fúster *et al.*, 1968). Its most important geomorphological feature is the development of 'jable' (De La Nuez *et al.*, 1997). Three aeolian localities have been studied and sampled (Figs 1 and 5; Table 1): Morros Negros (GMN), Caleta del Sebo (GCS) and La Cocina (GLC) stratigraphic sections.

Montaña Clara is the smallest islet (1.1 km^2). It is made up of Upper Pleistocene and Holocene volcanic deposits (Fúster *et al.*, 1968; De La Nuez *et al.*, 1997). The non-volcanic Quaternary deposits consist of talus debris and dunes containing abundant land snail shells and hymenopter nests. The best-exposed aeolian deposits belong to the Caleta de Guzmán section (MCG) (Figs 1 and 5; Table 1).

Alegranza is the craggiest islet and, therefore, the 'jable' is less developed than on the other islets. The Montaña Lobos section (AML) (Figs 1 and 5; Table 1) has been studied and sampled. Only a thin palaeosol has been observed at the top of the section, being capped by pyroclastic materials from recent volcanic eruptions of 'La Caldera' (Fig. 5).

Material and methods

Amino acid racemisation

For amino acid racemisation dating purposes samples were collected with gloves and tweezers, excavating 30–50 cm deep holes to avoid surface contamination and minimise the influence of air temperature. The sampled horizons are indicated for each stratigraphic section according to Figs 3 to 5 and Table 4. A total number of 237 Helicidae samples were

Table 1 Geographical location of the sections

Island Islet	Section	Nomenclature	Longitude	Latitude	Elevation (m)
	Barranco de Encantados	FBE	28° 38′ 12″ N	13° 59′ 4″ W	153
	Montaña de la Costilla	FMC	28° 41′ 16″ N	13° 58′ 9″ W	55
Fuerteventura	Barranco del Pecenescal	FBP	28° 7′ 42″ N	14° 16′ 49″ W	95
	Atalayeja Grande	FAG	28° 8′ 53″ N	14° 17′ 18″ W	237
	Montaña Azufrá	FMA	28° 5′ 41″ N	14° 27′ 52″ W	90
	Hueso del Caballo	FHC	28° 10′ 17″ N	14° 14′ 33″ W	100
	Lomo de San Andrés	LLA	29° 2′ 12″ N	13° 36′ 48″ W	280
Lanzarote	Tao	LTA	29° 2′ 36″ N	13° 36′ 51″ W	247
	Mala	LMA	29° 5′ 43″ N	13° 27′ 38″ W	25
	Morros Negros	GMN	29° 15′ 22″ N	13° 29′ 16″ W	10
La Graciosa	Caleta del Sebo	GCS	29° 13′ 38″ N	13° 30′ 12″ W	2
	La Cocina	GLC	29° 13′ 8″ N	13° 32′ 6″ W	25
Montaña Clara	Caleta de Guzmán	MCG	29° 16′ 35″ N	13° 31′ 46″ W	3
Alegranza	Montaña Lobos	AML	29° 23′ 20″ N	13° 30′ 10″ W	30

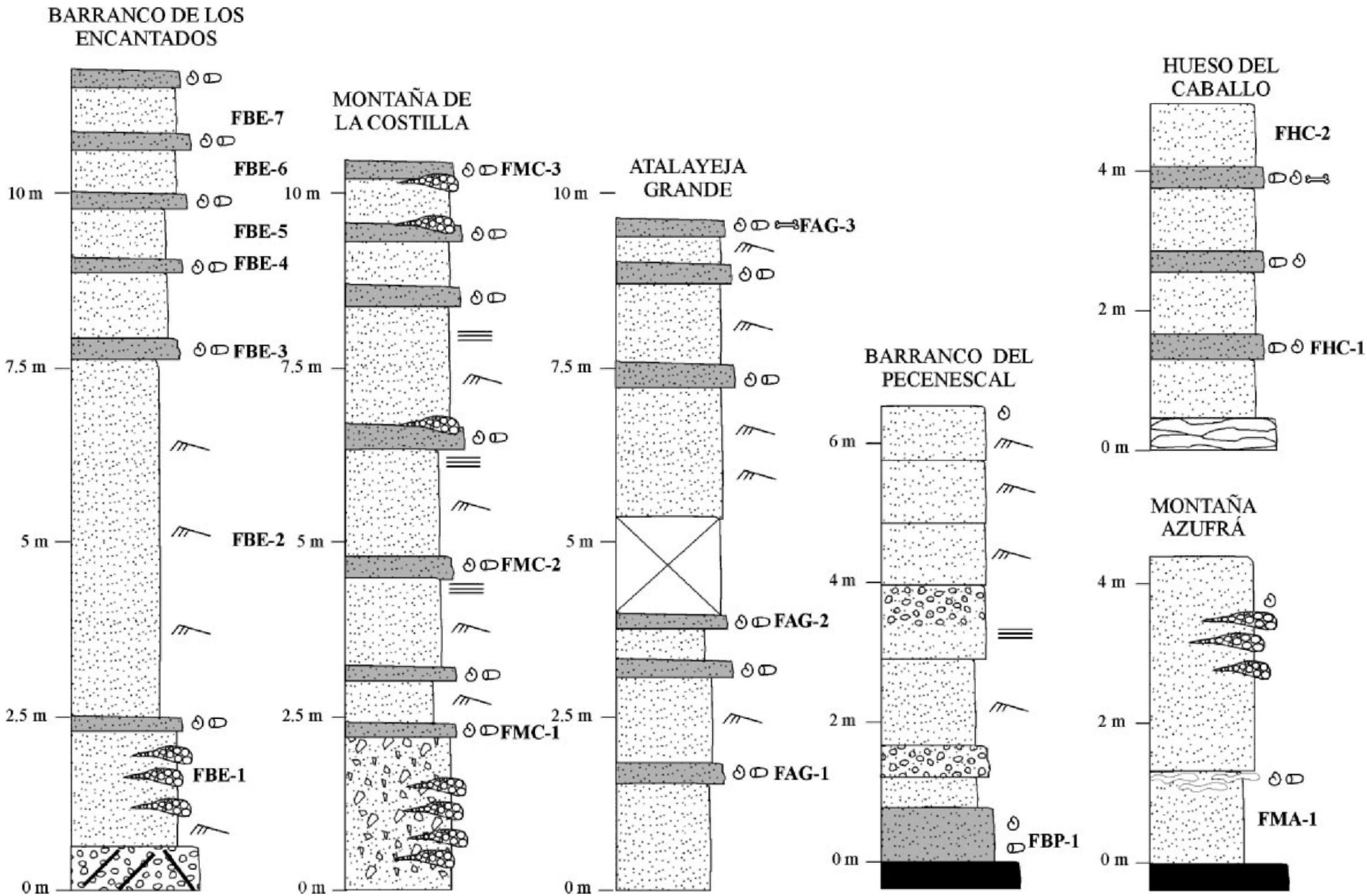

Figure 3 Composite stratigraphic sections of Fuerteventura Island: Barranco de los Encantados (FBE), Montaña de la Costilla (FMC), Barranco del Pecenescal (FBP), Atalayeja Grande (FAG), Montaña Azufrá (FMA), and Hueso del Caballo (FHC). The sampled horizons are shown. For legend see Fig. 4

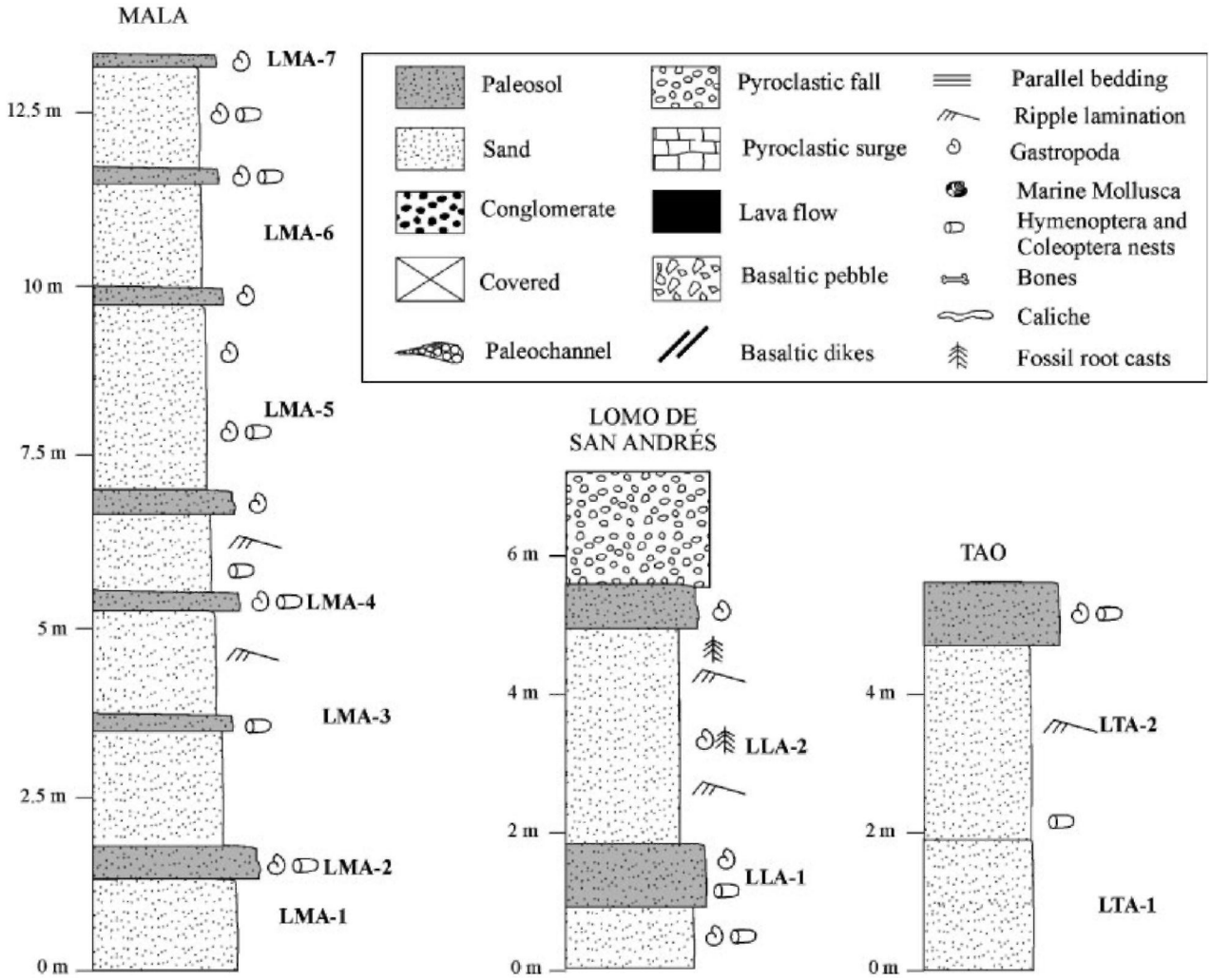

Figure 4 Composite stratigraphic sections of Lanzarote Island: Mala (LMA), Loma de San Andrés (LLA), and Tao (LTA). Sampled horizons are shown

analysed, belonging to *Theba geminata* (Mousson) and, in one locality (MCG-1), *Theba arinagae* Gittenberger and Ripken. This genus was selected because it is the most abundant endemic one on the eastern Canary Islands (Gittenberger and Ripken, 1987; Gittenberger *et al.*, 1992; Castillo *et al.*, 2002). In order to establish the lack of diagenesis in the shells, X-ray diffraction studies were carried out, showing an aragonitic composition, similar to the actual representatives (unpublished data). Both species were used together because only monogeneric samples produce taxonomically controlled variability in D/L ratios (Murray-Wallace, 1995; Murray-Wallace and Goede, 1995). Three living gastropods were also analysed to establish the induced racemisation by the acid-hydrolysis during sample preparation.

Samples were sieved under running water and dried at room temperature. Gastropods were carefully sonicated and cleaned with water to remove the sediment contained inside the shells. Afterwards, they were cleaned in 2 N HCl and 70–80 mg of shell was selected.

The sample preparation protocol is described in Goodfriend (1991) and Goodfriend and Meyer (1991) and involves:

1 Hydrolysis under N_2 atmosphere in a mixture of 12 N HCl (2.9 µl/mg) and 6 N hydrochloric acid (100 µl) for 20 h at 100 °C; desalting with HF, freezing and drying of the supernatant under vacuum.
2 Derivatisation: amino acids were derivatised in a two-step process, first involving esterification with 250 µl of 3 M thionyl chloride in isopropanol for 1 h at 100 °C under N_2; the samples were dried and acylated by reaction with 200 µl of trifluoroacetic acid anhydride (25% in dichloromethane) for 5 min at 100 °C. Excesses of derivative and solvent were evaporated under a gentle flow of nitrogen. The sample was taken up in 100 µl of *n*-hexane.

1 µl was injected into a Hewlett-Packard 5890 gas chromatograph. The injection port was kept at 215 °C and set for splitless mode for the first 75 s, at the beginning of which the sample was injected, and later set to split mode. Helium was used as the carrier gas, at a column head pressure of 5.8 psi, with a Chirasil-L-Val fused silica column (0.39 mm × 0.25 µm × 25 m) from Chrompack. The gradients used were as follows: 50 °C (1 min), heating at 40 °C/min to 115 °C, 12 min at 115 °C, heating at 3 °C/min to 190 °C, 10 min at 190 °C, cooling to 50 °C and remaining at this temperature between runs (at 80 °C if the time between runs was longer, typically overnight). The detector used was an NPD set at 300 °C. Integration of the peak areas was carried out using the HP PEAK96 integration program from Hewlett-Packard.

Radiocarbon dating

Three samples (GMN-3, GCS-1 and MCG-1) were previously dated in the Gliwice Radiocarbon Laboratory of the Silesian

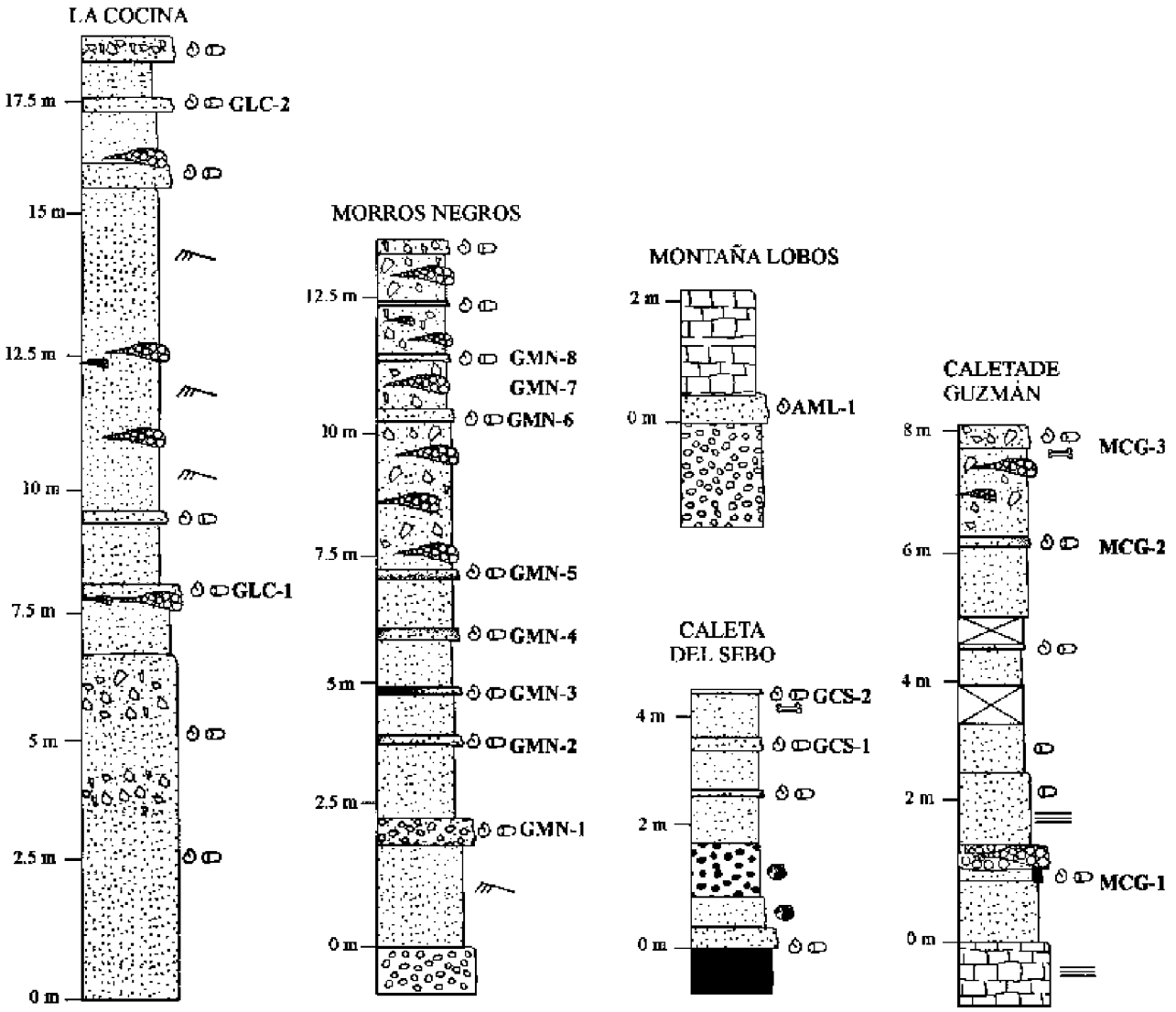

Figure 5 Composite stratigraphic sections of Chinijo Archipelago: Morros Negros (GMN), Caleta del Sebo (GCS), La Cocina (GLC), Caleta de Guzmán (MCG) and Montaña Lobos (AML). The sampled horizons are shown. For legend see Fig. 4

University of Technology (Poland) by De La Nuez *et al.* (1997) using the conventional radiometric technique (Table 6).

Additional AMS radiocarbon dating was undertaken on gastropods from new collections from samples MGC-3, FMC-1, FMC-3, FAG-1, FAG-3, LMA-2, LMA-7, and LLA-2 in the Gliwice Radiocarbon Laboratory. The gastropods were treated with 0.5 M HCl in order to remove the surface layer of carbonate. Afterwards, the $CaCO_3$ was decomposed with concentrated H_3PO_4, and released CO_2 was collected, purified and graphitised. Radiocarbon concentration in produced graphite targets was measured with use of a NEC Compact Carbon AMS system.

Table 2 Correlation coefficients (r) between D/L ratios of various amino acids from *Theba* shells recovered in the eastern islands and islets of the Canary Archipelago. All correlations are statistically significant at the level of $p < 0.001$

	D-alle/L-Ile	D/L Asp	D/L Phe	D/L Glu
D-alle/L-Ile	—	0.796	0.800	0.959
D/L Asp		—	0.833	0.857
D/L Phe			—	0.829

D-alle/L-Ile: D-alloisoleucine/L-isoleucine; Asp: aspartic acid; Phe: phenylalanine; Glu: glutamic acid.

Results and discussion

The D/L ratios of four amino acids (isoleucine, aspartic acid, phenylalanine and glutamic acid), obtained from 237 analytical samples of *Theba* from the eastern islands and islets of the Canary Archipelago, correlate strongly with each other (Table 2) and can be directly related to the age of the sampled horizon. The D/L ratios of leucine, alanine or valine, however, do not behave similarly. They show low correlation coefficients, which suggests that not only age but also other factors affect their racemisation ratios (Goodfriend, 1991).

The covariance patterns of the D/L ratios were analysed by principal components analysis (Table 3). The first component axis (eigenvector) accounts for ca. 96% of the covariation of the D/L ratios, which represents the covariation in racemisation/epimerisation rates in the four amino acids measured in *Theba* shells. This is why we used the D/L ratios of the four amino acids together to establish the aminostratigraphy and aminochronology of the aeolian deposits. In fact, according to Goodfriend (1991), the analysis of more than one amino acid

Table 3 Principal components analysis of the correlation matrix of the D/L ratios of the four amino acids measured in *Theba* samples described in Table 4, giving the first three eigenvectors (principal component axis) and the proportion of the total variance in the data set

	Eigenvector 1	Eigenvector 2	Eigenvector 3
D-alle/L-Ile	0.949	0.279	−0.087
D/L Asp	0.923	−0.197	0.329
D/L Phe	0.911	−0.312	−0.269
D/L Glu	0.968	0.207	0.025
Proportion of variance	88.02	6.40	4.70

D-alle/L-Ile: D-alloisoleucine/L-isoleucine; Asp: aspartic acid; Phe: phenylalanine; Glu: glutamic acid.

provides largely redundant information on sample age. The mean D/L ratios of the different amino acids (isoleucine, aspartic acid, phenylalanine and glutamic acid) in *Theba* shells are given in Table 4.

Aminostratigraphy

Aminostratigraphy consists in 'placing in stratigraphic order' sets of geological or palaeontological localities according to the D/L ratios measured from the same group of fossils (genera). Fundamental to this exercise is the assumption that all samples of the same age are preserved under similar environmental conditions, inorganic geochemistry and thermal histories. Therefore, each aminozone constitutes a dune/palaeosol formation event.

Table 4 Mean values and standard deviation of D/L ratios of isoleucine, aspartic acid, phenylalanine and glutamic acid obtained in *Theba* shells from the eastern islands and islets of the Canary Archipelago and summary of the datings. *n*: number of samples analysed

Sample	*n*	D-alle/L-Ile	D/L Asp	D/L Phe	D/L Glu	Age (ka BP)
Actual	3	0.001 ± 0.000	0.037 ± 0.013	0.020 ± 0.002	0.022 ± 0.002	—
FBP-1	5	0.293 ± 0.033	0.492 ± 0.045	0.436 ± 0.045	0.269 ± 0.029	15.2 ± 3.4
FBE-1	5	0.855 ± 0.113	0.669 ± 0.051	0.695 ± 0.077	0.580 ± 0.075	48.1 ± 5.6
FBE-2	5	0.888 ± 0.056	0.647 ± 0.049	0.703 ± 0.029	0.564 ± 0.044	47.8 ± 5.7
FBE-3	5	0.839 ± 0.056	0.635 ± 0.065	0.748 ± 0.045	0.534 ± 0.070	46.6 ± 6.5
FBE-4	5	0.729 ± 0.042	0.593 ± 0.041	0.667 ± 0.053	0.533 ± 0.022	38.9 ± 6.4
FBE-5	5	0.659 ± 0.020	0.655 ± 0.059	0.654 ± 0.045	0.483 ± 0.043	37.6 ± 4.9
FBE-6	5	0.658 ± 0.026	0.628 ± 0.015	0.674 ± 0.036	0.493 ± 0.020	37.5 ± 4.2
FBE-7	5	0.622 ± 0.008	0.641 ± 0.033	0.637 ± 0.064	0.504 ± 0.019	39.3 ± 5.5
FHC-1	5	0.537 ± 0.088	0.544 ± 0.067	0.559 ± 0.014	0.409 ± 0.048	27.0 ± 4.5
FHC-2	5	0.431 ± 0.026	0.578 ± 0.016	0.506 ± 0.059	0.341 ± 0.014	23.2 ± 4.2
FMA-1	5	0.602 ± 0.082	0.590 ± 0.044	0.537 ± 0.055	0.420 ± 0.069	29.7 ± 5.0
FMC-1	5	0.813 ± 0.017	0.640 ± 0.018	0.707 ± 0.045	0.555 ± 0.018	47.2 ± 4.6
FMC-2	5	0.761 ± 0.045	0.669 ± 0.045	0.680 ± 0.053	0.534 ± 0.040	44.7 ± 6.5
FMC-3	5	0.156 ± 0.044	0.416 ± 0.054	0.250 ± 0.020	0.168 ± 0.035	6.3 ± 2.4
FAG-1	5	0.830 ± 0.083	0.725 ± 0.070	0.719 ± 0.088	0.628 ± 0.064	55.7 ± 5.5
FAG-2	5	0.388 ± 0.019	0.562 ± 0.022	0.520 ± 0.034	0.317 ± 0.014	21.6 ± 4.4
FAG-3	5	0.163 ± 0.011	0.330 ± 0.033	0.195 ± 0.024	0.134 ± 0.020	5.4 ± 1.7
LTA-1	5	0.208 ± 0.018	0.434 ± 0.046	0.401 ± 0.063	0.231 ± 0.035	11.8 ± 4.0
LTA-2	5	0.220 ± 0.024	0.470 ± 0.010	0.411 ± 0.021	0.239 ± 0.028	12.3 ± 2.8
LLA-1	5	0.682 ± 0.077	0.627 ± 0.037	0.660 ± 0.043	0.488 ± 0.037	38.0 ± 4.0
LLA-2	5	0.576 ± 0.053	0.630 ± 0.023	0.632 ± 0.041	0.427 ± 0.033	33.5 ± 3.2
LMA-1	5	0.684 ± 0.082	0.638 ± 0.046	0.639 ± 0.070	0.502 ± 0.041	38.6 ± 6.9
LMA-2	5	0.625 ± 0.026	0.666 ± 0.025	0.668 ± 0.038	0.502 ± 0.023	39.8 ± 4.6
LMA-3	5	0.590 ± 0.027	0.624 ± 0.031	0.667 ± 0.026	0.438 ± 0.019	34.9 ± 5.3
LMA-4	10	0.538 ± 0.049	0.612 ± 0.017	0.597 ± 0.029	0.416 ± 0.034	30.6 ± 4.2
LMA-5	5	0.547 ± 0.052	0.603 ± 0.012	0.602 ± 0.030	0.429 ± 0.018	31.1 ± 3.2
LMA-6	5	0.435 ± 0.029	0.566 ± 0.034	0.602 ± 0.062	0.356 ± 0.024	27.4 ± 4.4
LMA-7	5	0.450 ± 0.033	0.604 ± 0.029	0.595 ± 0.047	0.390 ± 0.014	28.2 ± 5.1
GMN-1	6	0.720 ± 0.042	0.679 ± 0.065	0.643 ± 0.063	0.534 ± 0.053	43.0 ± 7.8
GMN-2	6	0.725 ± 0.039	0.673 ± 0.045	0.673 ± 0.040	0.554 ± 0.047	43.6 ± 6.3
GMN-3	6	0.734 ± 0.071	0.671 ± 0.033	0.661 ± 0.038	0.520 ± 0.032	42.2 ± 5.2
GMN-4	5	0.679 ± 0.027	0.661 ± 0.030	0.656 ± 0.057	0.506 ± 0.020	40.2 ± 4.8
GMN-5	6	0.801 ± 0.042	0.676 ± 0.024	0.665 ± 0.032	0.516 ± 0.038	43.5 ± 4.9
GMN-6	5	0.518 ± 0.067	0.614 ± 0.028	0.554 ± 0.080	0.406 ± 0.029	29.4 ± 4.6
GMN-7	5	0.261 ± 0.032	0.498 ± 0.038	0.480 ± 0.054	0.264 ± 0.012	16.5 ± 3.9
GMN-8	5	0.272 ± 0.051	0.489 ± 0.037	0.416 ± 0.067	0.252 ± 0.079	17.6 ± 3.3
GCS-1	6	0.452 ± 0.017	0.626 ± 0.032	0.624 ± 0.049	0.384 ± 0.019	30.3 ± 5.5
GCS-2	6	0.360 ± 0.045	0.565 ± 0.019	0.492 ± 0.042	0.316 ± 0.014	20.6 ± 3.4
GLC-1	5	0.537 ± 0.037	0.594 ± 0.068	0.616 ± 0.042	0.414 ± 0.034	31.5 ± 5.7
GLC-2	4	0.457 ± 0.040	0.564 ± 0.047	0.510 ± 0.051	0.391 ± 0.029	24.8 ± 4.4
MCG-1	6	0.698 ± 0.084	0.670 ± 0.049	0.644 ± 0.076	0.535 ± 0.049	40.2 ± 7.9
MCG-2	5	0.473 ± 0.061	0.611 ± 0.064	0.583 ± 0.089	0.415 ± 0.057	28.5 ± 6.4
MCG-3	6	0.113 ± 0.005	0.319 ± 0.007	0.188 ± 0.077	0.157 ± 0.068	4.6 ± 0.7
AML-1	5	0.115 ± 0.023	0.472 ± 0.059	0.373 ± 0.053	0.176 ± 0.021	10.1 ± 4.0

D-alle/L-Ile: D-alloisoleucine/L-isoleucine; Asp: aspartic acid; Phe: phenylalanine; Glu: glutamic acid.

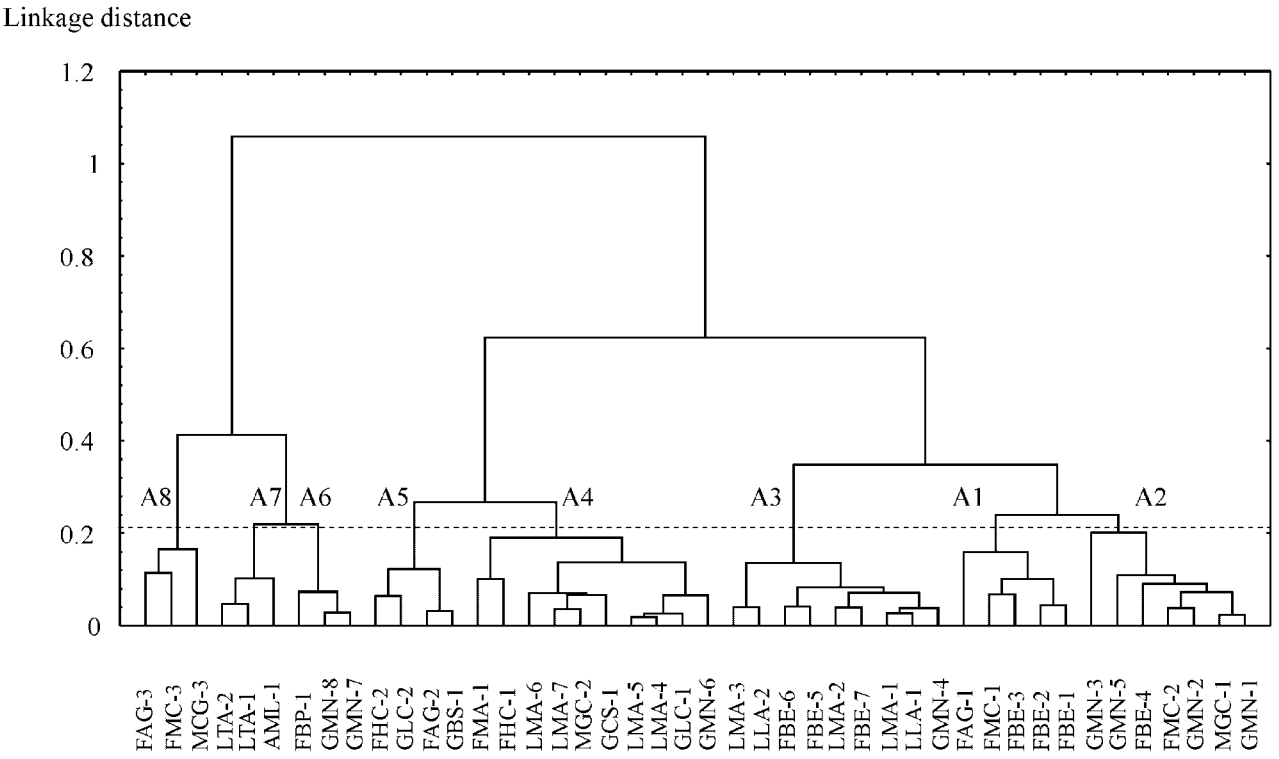

Figure 6 Dendrogram (complete linkage and Euclidean distance) of the D-alle/L-Ile, D/L Asp, D/L Phe and D/L Glu values obtained in *Theba* snails from diverse stratigraphic sections of the Canary Archipelago eastern islands. Each cluster was identified to an aminozone (A1, oldest, to A8, youngest)

Eight groups (aminozones) were established with the aid of cluster analysis (complete linkage and Euclidean distance), using the isoleucine, aspartic acid, phenylalanine and glutamic acid D/L ratios (Fig. 6). The mean D/L ratios of each aminozone are in Table 5. Aminozone 1, with the highest racemisation/epimerisation ratios, groups the oldest deposits (earliest dune/palaeosol-formation episode found on these islands), while Aminozone 8 corresponds to the youngest beds (eighth dune/palaeosol-formation episode).

In order to test the reliability of the aminozones we performed multivariate analysis of variance (MANOVA). We compared the mean square values through the variance ratio *F* test. The results in Table 7 show that the significance level (*p*) is much lower than 0.01. Likewise, the observed value of *F* (24.87) is greater than the tabulated value (1.65) at the 95% level of confidence and also greater than the tabulated *F* value (2.06) at the 99% level of confidence, so the null hypothesis (similarity of aminozones) can be rejected. Furthermore, the Wilks' lambda value is 0.079, close to 0, meaning that a good discrimination can be interpreted between aminozones. Therefore, the MANOVA does clearly distinguish between the mean D/L ratios of isoleucine, aspartic acid, phenylalanine and glutamic acid that define the aminozones. We also calculated the squared Mahalanobis distances between the group centroids to compare the mean response between pairs of aminozones. The Mahalanobis distance is similar to the standard Euclidean distance measure, except that it takes into account the correlations between variables. The respective *p*-levels of the squared Mahalanobis distances between pairs of aminozones (Table 8) are below 0.05 (most of them even below 0.01) and, therefore, the mean D/L values that define each aminozone are reliable.

There is close correspondence between the aminozones and the stratigraphic position of the beds within each section (Fig. 7). According to these results, the lower half of the Barranco de los Encantados section (from FBE-1 to FBE-3) corresponds to the same (and oldest) dune-formation episode, and correlates with the bottom of the Montaña de la Costilla (FMC-1) and Atalayeja Grande sections (FAG-1), all of which are located on Fuerteventura Island (Fig. 7).

Table 5 Mean and standard deviation values of isoleucine, aspartic acid, phenylalanine and glutamic acid D/L ratios that characterise the aminozones established in the eastern islands and islets of the Canary Archipelago. The average age of the different aminozones is also represented

Aminozones	D-alle/L-Ile	D/L Asp	D/L Phe	D/L Glu	Age (ka)
8	0.139 ± 0.018	0.343 ± 0.029	0.201 ± 0.030	0.152 ± 0.030	5.4 ± 1.1
7	0.173 ± 0.056	0.459 ± 0.044	0.384 ± 0.051	0.209 ± 0.040	11.0 ± 4.0
6	0.270 ± 0.034	0.505 ± 0.035	0.443 ± 0.051	0.262 ± 0.025	14.9 ± 3.6
5	0.402 ± 0.039	0.568 ± 0.026	0.510 ± 0.037	0.337 ± 0.035	22.4 ± 4.5
4	0.589 ± 0.064	0.603 ± 0.037	0.586 ± 0.040	0.395 ± 0.040	29.4 ± 4.8
3	0.643 ± 0.055	0.640 ± 0.034	0.653 ± 0.040	0.484 ± 0.038	37.8 ± 4.6
2	0.741 ± 0.053	0.659 ± 0.044	0.658 ± 0.039	0.529 ± 0.037	42.5 ± 6.0
1	0.834 ± 0.059	0.677 ± 0.050	0.719 ± 0.062	0.576 ± 0.060	48.6 ± 6.4

D-alle/L-Ile: D-alloisoleucine/L-isoleucine; Asp: aspartic acid; Phe: phenylalanine; Glu: glutamic acid.

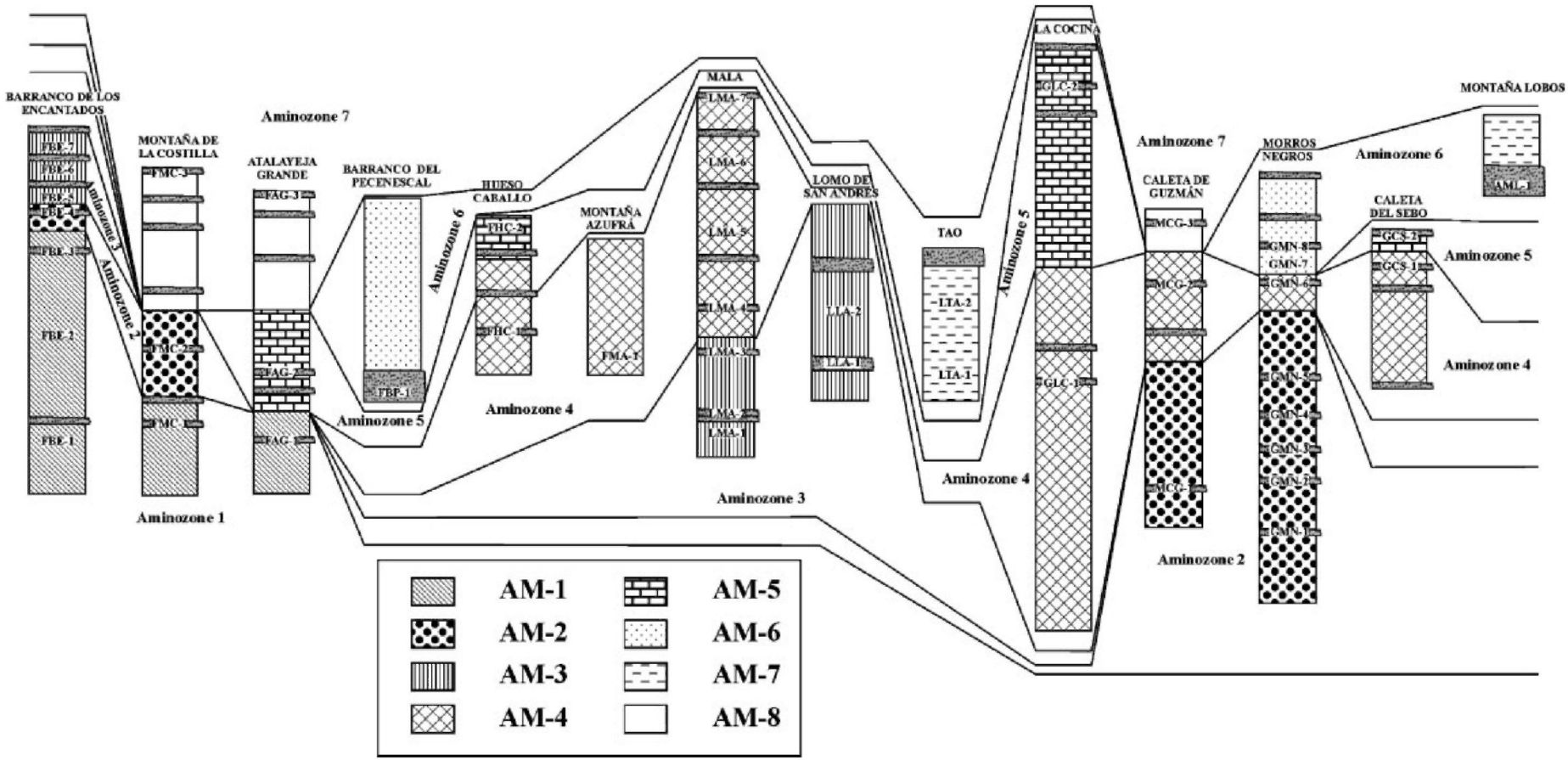

Figure 7 Aminostratigraphical correlation between the stratigraphic sections from the eastern islands and islets of the Canary Archipelago. The position of the palaeosols are plotted in each section

The lower half of the Morros Negros (La Graciosa Islet) stratigraphic section, from set GMN-1 to GMN-5 with the exception of set GMN-4, belongs to Aminozone 2, and correlates with the bottom of Caleta de Guzmán (MCG-1), located at Montaña Clara Islet, and the middle part of the Barranco de los Encantados (FBE-4) and Montaña de la Costilla (FMC-2) sections, both on Fuerteventura Island (Fig. 7). It is noticeable that set GMN-4, which should be included within Aminozone 2, belongs to Aminozone 3. This is due to the lower isoleucine D/L value in GMN-4 than in beds GMN-1, 2, 3 and 5, while the racemisation ratios of aspartic acid, phenylalanine and glutamic acid are similar.

The top half of the Barranco de los Encantados section (FBE-5 to FBE-7) was deposited during the third dune-formation episode, together with beds from the Loma de San Andrés section (LLA-1 and 2) and the bottom of the Mala section (LMA-1 to 3), both from Lanzarote Island (Fig. 7).

The bottom of the Montaña Azufrá section (FMA-1) and the bottom of the Hueso del Caballo section (FHC-1), both on Fuerteventura, correspond to the fourth dune-formation episode (Fig. 7). These beds correlate with the top half of the Mala section (LMA-4 to 7), the middle of the Caleta de Guzmán section (bed MCG-2), the bottom of the Caleta del Sebo section (CGS-1), the bottom of the La Cocina section (GLC-1) and set GMN-6 of the Morros Negros section (Fig. 7).

During the fifth dune-formation episode, the top of the Hueso del Caballo (FHC-2), La Cocina (GLC-2) and Caleta del Sebo (GCS-2) sections were deposited, as well as the intermediate beds of Atalayeja Grande section (FAG-2) (Fig. 7).

The Tao section (LTA-1, 2) and the Montaña Lobos section (AML-1) are grouped in Aminozone 6 (Fig. 7).

The top of the Morros Negros section (GMN-7, 8) and at least the bottom of the Barranco del Pecenescal (FBP-1) section were deposited during the seventh dune-formation episode (Fig. 7).

Unfortunately, the top of the Barranco del Pecenescal section was strongly cemented and no amino acid racemisation analysis on gastropods could be performed. We cannot rule out the possibility that the uppermost part of this section belongs to Aminozone 8, which includes the top of the Atalayeja Grande (FAG-3), Montaña de la Costilla (FMC-3) and Caleta de Guzmán (MGC-3) sections (Fig. 7).

These results demonstrate that all the dune-palaeosol accumulation episodes (aminozones) are nowhere recorded in the same stratigraphic section. In some cases, there was a continuity of several successive episodes (FBE, FHC, LMA, GCS and GLC sections), whereas in other sections the amino acid ratios suggest the presence of a hiatus (FAG, FMC, GMN and MCG sections). In sections AML, LLA, LTA, FBP and FMA, only one dune-formation episode is recorded.

The highly similar values of the D/L ratios (e.g. around 0.73 in D-alle/L-Ile) of the different amino acids in samples from palaeosols 1 to 5 of the GMN section suggest the stacking of dune beds between periods of soil formation over a short period of time. This alternating pattern of dunes and palaeosols implies a rapid change in environmental conditions, from more arid stages represented by mobile dunes to more humid phases represented by palaeosols. This style of deposition also occurs in other aeolian formations on the island of Lanzarote, where a D-alle/L-Ile ratio of $\sim$0.5 obtained in six stacked palaeosols of a stratigraphic section (Hillaire-Marcell *et al.*, 1995) indicates rapid deposition. The greatest variations in the D/L ratios are found between palaeosols MCG-2 and MGC-3 on the islet of Montaña Clara, pointing to a period of dune activation that should be much longer than the formation timespan of the first five palaeosol levels of Morros Negros.

Aminochronology

Aminochronology is a means of converting the relative D/L ratios of the amino acids into numerical ages. However, the amino acid racemisation method is not a numerical dating method in itself and needs to be calibrated with either previously dated samples (i.e. through radiometric dating methods) or by 'high'-temperature laboratory experiments to determine the rate of natural amino acid racemisation/epimerisation in a particular genus.

As the racemisation process is both genus- and temperature-dependent, age calculation algorithms can only be established from samples located in areas with the same thermal history, e.g. *Theba* shells recovered in the Canary Islands. Two models are commonly used for calibration: first-order reversible kinetics (FOK) and apparent parabolic kinetics (APK).

For calibration, several dated samples of different ages are needed. When previously dated samples are scarce, the calibration can be simplified by taking an FOK pattern (Mitterer, 1975) that relates the expression $\ln[(1 + D/L)/(1 - D/L)]$ with time or the square root of time. According to some authors, the racemisation/epimerisation reaction is presumed to follow reversible FOK kinetics only at initial stages of diagenesis (Masters and Bada, 1977; Kriausakul and Mitterer, 1980; Miller and Brigham-Grette, 1989; Wehmiller and Hare, 1971; Bada and Schroeder, 1972). Nevertheless, the best correlations between D/L ratios (up to 1.0) of different amino acids and time and/or the square root of time were obtained with FOK by Miller *et al.* (1991, 1992), Torres *et al.* (1997) and Ortiz *et al.* (2004).

Mitterer and Kriausakul (1989) modelled racemisation/epimerisation reactions in terms of APK, a procedure that generates a linear relationship between the square root of time and D/L ratios. However, the applicability of the parabolic approach at very low or high D/L ratios may be questionable (Mitterer and Kriausakul, 1989; Murray-Wallace and Kimber, 1993). Other relationships between age and D/L ratios have also been proposed (Goodfriend *et al.*, 1992, 1995; Ellis *et al.*, 1996; Csapò *et al.*, 1998; Kaufman, 2000; Manley *et al.*, 2000).

In short, since no model seems to describe satisfactorily the patterns of each of the amino acids, a model must be chosen empirically for each data set based on the goodness of fit (Goodfriend, 1991). In fact, in the studies by Goodfriend (1991) and Ortiz *et al.* (2004), the patterns of some amino acids linearised better with apparent parabolic kinetics, while for others the 'first-order kinetics' trend was the best one. For the calculation of algorithms, the radiocarbon data of Table 6 were used. It must not be overlooked that in carbonate areas, land snails ingest old carbonates (deficient in ^{14}C) and incorporate this carbon into their shells during growth (Goodfriend and Hood, 1983). Thus, ages can be anomalously old and range up to ca. 3 ka (Goodfriend and Stipp, 1983; Goodfriend, 1987b; Goodfriend *et al.*, 1999). This age anomaly can be calculated from radiocarbon analysis of modern, live-collected shells or shells collected alive before thermonuclear bomb tests in the 1950s.

In our case, we used the age anomaly of an actual gastropod (*Theba*) from the Canary Islands (Table 9). For the calculation of the age anomaly of the live-collected gastropod Goodfriend's (1987a) equation was employed:

$$A'_m = A_m \left[1 - \frac{2\left(\frac{\delta^{13}C}{A_m/A_a} + 25\right)}{1000} \right]$$

Table 6 ^{14}C datings of fossil gastropod samples from the stratigraphic sections studied from the eastern Canary Islands. Analysis of GMN-3, GCS-1, and MCG-1 were obtained by De La Nuez *et al.* (1997) using a conventional radiocarbon technique. Analysis of the rest of the samples were performed in an AMS. See text for details of correction procedures

Sample	Material	^{14}C age (yr BP)	Corrected ^{14}C age (yr BP)	Calibrated age (yr BP)
MCG-3	GdA-391	5770 ± 35	3046 ± 47	3250 ± 70
FMC-3	GdA-379	6260 ± 40	3536 ± 51	3810 ± 70
FAG-3	GdA-383	6960 ± 40	4236 ± 51	4750 ± 90
GCS-1	Gd-10441	33 600 ± 1400	30 876 ± 1400	36 160 ± 1780
MCG-1	Gd-10439	36 200 + 2600 − 2000	33 776 ± 2300	38 890 ± 2240
LMA-7	GdA-386	37 700 ± 500	34 976 ± 500	40 760 ± 790
GMN-3	Gd-10438	37 800 + 3300 − 2400	35 526 ± 2850	39 820 ± 2460
FMC-1	GdA-378	40 600 ± 600	37 876 ± 600	42 530 ± 270
FAG-1	GdA-382	42 200 ± 700	39 476 ± 700	43 320 ± 450
LMA-2	GdA-385	43 000 ± 800	40 276 ± 800	43 810 ± 580
LLA-2	GdA-387	43 300 ± 800	40 576 ± 800	44 000 ± 630

Table 7 Multivariate analysis of variance (MANOVA) of the isoleucine, aspartic acid, phenylalanine and glutamic acid D/L ratios from the amino-zones established in the eastern islands and islets of the Canary Archipelago

Wilks' *lambda*	Observed *F*	d.f.	Tabulated *F* (for $\alpha = 0.05$)	Tabulated *F* (for $\alpha = 0.01$)	*p*-level
0.0792	24 879	(28 900)	1.65	2.06	< 0.0001

d.f. degrees of freedom.

Table 8 *p*-levels of the squared Mahalanobis distances among the amino acid D/L ratios of pairs of Aminozones

Compared aminozones	*p*-level
Am 7 vs. Am 8	0.00557
Am 6 vs. Am 7	0.00253
Am 5 vs. Am 6	0.00925
Am 4 vs. Am 5	0.00974
Am 3 vs. Am 4	< 0.00001
Am 2 vs. Am 3	< 0.00001
Am 1 vs. Am 2	< 0.00001

where A_m is the measured ^{14}C activity of the shell and A_a is the contemporary atmospheric ^{14}C activity.

The estimated age anomaly is 2724 ± 32 yr and was used to correct the ages obtained in the fossil *Theba* samples. The age anomaly was subtracted from the measured ^{14}C ages of fossil samples and then the variance was added to the reported analytical variance in ^{14}C age to obtain the overall uncertainty of ^{14}C age ($\sigma_{total} = \sqrt{32^2 + \sigma^2}$). We then converted these corrected radiocarbon ages into calendar years using the Radiocarbon Calibration Program 4.4 (CALIB 4.4) (Stuiver and Reimer, 1993) with the calibration dataset of Stuiver *et al.* (1998) for Holocene samples (Table 6). The correction of the age anomaly of samples older than 30 k ^{14}C yr BP was performed with the CAL_PAL program (Weninger *et al.*, 2004) with the calibration dataset CalPal2004_SFCP (Table 6).

For establishing age calculation algorithms through the amino acid racemisation/epimerisation ratios, we first used all the samples of Table 6. However, we found that these equations provided ages for samples FAG-1, LLA-2 and LMA-7 that differed from ages obtained with radiocarbon dating. Because of this, we rejected samples FAG-1, LLA-2 and LMA-7 for the calculation of the models.

To select the best fit for the amino-age estimation algorithms, we compared the correlation coefficients (r) for various approaches (Table 10). We chose to use the following relationships because they provided the highest correlation coefficients: D-alle/L-Ile values versus time (APK); the phenylalanine and glutamic acid D/L ratios versus square root of time (APK); and the first-order kinetic transformation of the aspartic acid D/L ratios versus square root of time (Table 10). The results are (Fig. 8):

For isoleucine:

$$t = -1.939 + 60.42 \text{ D-alle/L-Ile}$$

For aspartic acid:

$$\sqrt{t} = -0.9764 + 4.6177 \ln\left[\frac{1 + \text{D/L}}{1 - \text{D/L}}\right]$$

For phenylalanine:

$$\sqrt{t} = -0.1024 + 9.8306 \text{ D/L Phe}$$

For glutamic acid:

$$\sqrt{t} = 0.10427 + 12.322 \text{ D/LGlu}$$

Numerical dating was obtained by introducing into the algorithms the *Theba* D/L ratios measured for each amino acid. The age is the average of the numerical dates obtained for each amino acid D/L ratio measured in analytical samples of a single bed (Table 4). Age uncertainty is the standard deviation of all

Table 9 Radiocarbon analyses of a live-collected *Theba* shell from the Canary Islands. PMC = % modern carbon. The contemporary ^{14}C value for comparison was taken from extrapolation of data in Levin and Hesshaimer (2000)

Laboratory no.	Collection yr	^{13}C (‰ PDB)	Shell ^{14}C ± SD (PMC)	Contemporary ^{14}C (PMC)	Relative shell ^{14}C (PMC)	Age anomaly (yr)
GdA-384	2002	4.4	76.01 ± 0.30	110	71.2	2724 ± 32

Table 10 Correlation coefficients (r) between time and D/L ratios of amino acids measured in *Theba* snail shells. Correlations are presented for: (1) D/L ratios transformed to first-order kinetics vs. time; (2) D/L ratios transformed to first-order kinetics vs. square root of time; (3) untransformed D/L ratios vs. time (APK); (4) untransformed D/L ratios vs. square root of time (APK). All correlations are statistically significant at the level of $p < 0.001$. The highest correlation coefficients are in bold

	1	2	3	4
D-alle/L-Ile	0.961	0.952	**0.968**	0.963
D/L Asp	0.933	**0.976**	0.907	0.962
D/L Phe	0.983	0.990	0.979	**0.994**
D/L Glu	0.972	0.972	0.974	**0.979**

D-alle/L-Ile: D-alloisoleucine/L-isoleucine; Asp: aspartic acid; Phe: phenylalanine; Glu: glutamic acid.

the numerical ages calculated from the amino acid D/L ratios. There was generally good correspondence between the ages calculated through amino acid racemisation and ages obtained by ^{14}C.

The average age of each aminozone was calculated by means of the numerical ages obtained from each isoleucine, aspartic acid, phenylalanine and glutamic acid D/L ratio of all the samples from each bed (Table 5). Despite the MANOVA and squared Mahalanobis distances demonstrating that the Aminozones are reliable, we performed a t-test analysis to determine whether the average ages of the Aminozones are significant (Table 11). The value of the p-level is the probability of error involved in acceptance of our observed result as valid, i.e. as representative of the population. The results show that, in all cases, p-levels are lower than 0.005 and the t values are higher than the tabulated t values for $\alpha = 0.05$ and $\alpha = 0.01$. Therefore, the average ages of the Aminozones are statistically highly significant.

According to these results, the dune-formation episodes all occurred between MIS 1 and 3, which is consistent with earlier studies. They can be described as events of aeolian deposit accumulation with a recurrence period of 5–7 ka. Each event occurred during arid conditions (De La Nuez *et al.*, 1997; Castillo *et al.*, 2002) and ended with the development of a palaeosol, which is interpreted as being caused by an increase in environmental moisture. These pulses of aeolian deposition are not exclusively related to a single sandy set, but to various dune beds capped by palaeosols.

Accumulations of aeolian sands interbedded with horizons of silt and clay (palaeosols) are common in coastal sequences of Mediterranean and subtropical North Atlantic regions. Previous work on amino acid racemisation/epimerisation measurements in land snail shells from aeolian formations has been performed by different authors: Hearty (1987) on the Island of Mallorca, Hearty *et al.* (1992) in Bermuda and Goodfriend *et al.* (1996) in Madeira. Dating of some of these sequences enables a comparison with the Canary Islands sections. However, the relationship between *Theba* snails D-alle/L-Ile ratios versus age obtained in the Canary Islands does not correlate with the data of *Helix* from Mallorca (Hearty, 1987), *Poecilozonites* from Bermuda (Hearty *et al.*, 1992) or *Actinella nitidiuscula, Caseolus bowdichianus, Geomitra delphinula* and *Leptaxis undata* from Madeira (Goodfriend *et al.*, 1996) (Table 12). Although different species were analysed in each study, as a helicid land snail, *Theba* would be expected to epimerise at rates not markedly different to those of the other species.

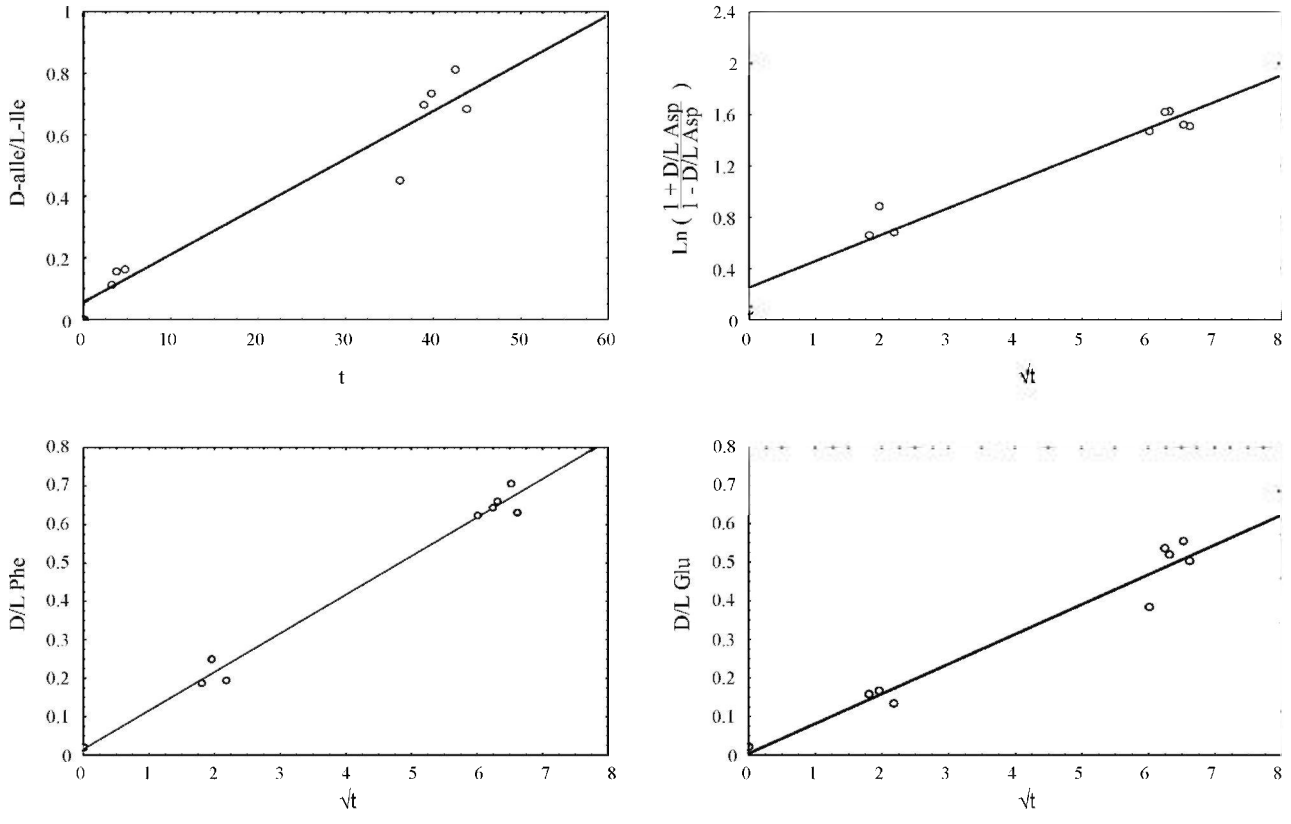

Figure 8 Plots of first-order kinetics transformed D/L ratios of land snail shells of the Canary Archipelago eastern islands versus square root of time for isoleucine, aspartic acid, phenylalanine and glutamic acid. D-alle/L-Ile: D-alloisoleucine/L-isoleucine; Asp: aspartic acid; Phe: phenylalanine; Glu: glutamic acid

Table 11 *t*-test analysis of the difference between the age means of the aminozones distinguished in the aeolian/palaeosol deposits from the Canary Islands. For comparison, the tabulated-*t* for $\alpha = 0.05$ is 1.96 and for $\alpha = 0.01$ is 2.57

Compared aminozones	*p*-level	d.f.	*t*-value
Am 7 vs. Am 8	<0.0001	258	6.067
Am 6 vs. Am 7	<0.0001	338	4.447
Am 5 vs. Am 6	<0.0001	402	9.312
Am 4 vs. Am 5	<0.0001	306	6.209
Am 3 vs. Am 4	<0.0001	142	10.063
Am 2 vs. Am 3	<0.0001	122	6.528
Am 1 vs. Am 2	<0.0001	126	5.372

d.f.: degrees of freedom = $N_1 + N_2 - 2$. *N*: sample size.

First of all, this discrepancy needs to be examined in terms of the techniques employed for amino acid analysis, i.e. data from Mallorca (Hearty, 1987) and Bermuda (Hearty *et al.*, 1992) were obtained with ion-exchange liquid chromatography (IE-LC), whereas data from the Canary Islands were measured by gas chromatography (GC). As we have noticed (Ortiz *et al.*, 2005), there are slight differences between D-alle/L-Ile ratios obtained by GC and by IE-LC. This is based on the analysis of samples from an inter-laboratory comparison exercise (cf. Wehmiller, 1984; Torres *et al.*, 1997). The isoleucine epimerisation (D-alle/L-Ile) values ranging between 0.45 and 1.1 obtained by IE-LC are approximately 0.10 lower than those obtained by GC in our laboratory, i.e. D-alle/L-Ile_{GC} = D-alle/L-$Ile_{IE\text{-}LC}$ + ca. 0.10. For lower D-alle/L-Ile values, the difference is between 0 and 0.05; however, even when allowing for this transformation, the values from these localities do not coincide either.

In the comparison with Mallorca, the lack of correspondence should be found in differences in the mean annual temperatures (MAT) of the islands (Table 13), as racemisation/epimerisation is a thermo-dependent process; Mitterer (1975) observed that epimerisation rate doubles for every ca. 4 °C increase. Mallorca has a MAT of 17.1 °C, while the eastern Canary Islands have MATs around 19.5 °C (Rivas-Martínez and Rivas y Sáenz, 2005) (Table 13). In fact, Hearty *et al.* (1986) found differences in D-alle/L-Ile values of as much as 0.12 in marine *Glycymeris* shells from the last interglacial between Mallorca (D-alle/L-Ile ~ 0.37), Morocco (D-alle/L-Ile ~ 0.46) and Tunisia (D-alle/L-ile ~ 0.49), which were attributed to different mean annual temperatures of 2 °C. Similarly, Hearty and Kaufman (2000) found differences of 0.12 in D-alle/L-Ile ratios measured in oolitic samples of the same age (MIS 5e) in islands 700 km apart in the North and South Bahamas, which was attributed to a warming gradient of 2 °C between these islands. Likewise,

Table 12 Comparison of D-alle/L-ile values and age of different aeolian formations in Mediterranean and subtropical North Atlantic islands

Locality	D-alle/L-ile	Age (ka BP)	Technique	Material	Reference
Canary Archipelago	0.40	ca. 23	GC	*Theba geminata* & *Theba arinagae*	This paper
	0.65	ca. 40	GC		
Canary Archipelago	0.50	ca. 38	IE-LC	*Helicella* sp.	Hillaire-Marcel *et al.* (1995)
Mallorca Island	0.35–0.40	ca. 125	IE-LC	*Helix* sp.	Hearty (1987)
Bermuda Island	0.50–0.62	ca. 125	IE-LC	*Poecilozonites* sp.	Hearty *et al.* (1992)
Madeira Island	0.30	ca. 46	GC	*Actinella nitidiuscula, Caseolus bowdichianus, Geomitra delphinula* & *Leptaxis undata*	Goodfriend *et al.* (1996)
	0.45	ca. 140			
Negev Desert	0.35	ca. 10	DA	*Trochoidea seetzeni* & *Sphincterochila* sp.	Goodfriend (1987a)

GC: Gas chromatography; IE-LC: ion exchange liquid chromatography; DA: Diomedex amino acid analyser.

Table 13 Climatic parameters of different climatological stations (Rivas-Martínez and Rivas y Sáenz, 2005). Data from Beer Sheva and Madeira Island stations come from www.worldclimate.com. The bioclimatic classification was established by Rivas-Martínez *et al.* (2004)

Region	Climatic station	Latitude	Longitude	Average temp. (°C)	Rainfall (mm)	I_c	I_o	T_p	Bioclimatic classification
Bermuda Islands	Kindley	32° 21′ N	64° 41′ W	21.7	1525	9.8	5.87	2598	Tropical pluvial
Madeira Islands	Madeira Island	33° 40′ N	16° 89′ W	18.5	640	6.7	2.39	2260	Temperate hyperoceanic submediterranean
Mallorca Island	Palma Mallorca	39° 33′ N	2° 44′ E	17.1	460	14.8	2.24	2050	Mediterranean pluviseasonal-oceanic
Canary Islands	Arrecife (Lanzarote Island)	28° 57′ N	13° 33′ W	20.2	139	7.2	0.57	2426	Mediterranean desertic oceanic
Canary Islands	Pto Rosario (Fuerteventura Island)	28° 27′ N	13° 52′ W	19.9	110	7.0	0.46	2426	Mediterranean desertic oceanic
Canary Islands	La Oliva (Fuerteventura Island)	28° 36′ N	13° 59′ W	19.0	108	7.4	0.47	2285	Mediterranean desertic oceanic
Negev Desert, Israel	Beer Sheva	31° 23′ N	34° 78′ E	19.6	178	14.9	0.63	2800	Mediterranean desertic oceanic

T_p: yearly positive temperature in tenths of 1°C, the sum of the monthly average temperature of those months whose average temperature is higher than 0°C. I_c: continentality index (yearly thermic interval = T_{max}–T_{min}) in °C, the number expressing the range between the average temperatures of the warmest (T_{max}) and coldest (T_{min}) months of the year. I_o: ombrothermic index. $I_o = (P_p/T_p) \times 10$. P_p is the yearly positive precipitation (in mm), that is, the total average precipitation of those months whose average temperature is higher than 0°C.

Goodfriend and Mitterer (1988) found differences in D-alle/L-Ile ratios of samples with the same age (ca. 30 ka) in two localities in Jamaica (D-alle/L-Ile = 0.25 for Coco site samples; D-alle/L-Ile = 0.51 for Green Grotto site samples), which were attributed to a 4 °C temperature difference between the two sites.

Not only temperature but moisture (rainfall rate) has to be considered in order to explain the differences found between Bermuda, Madeira and the Canary Islands, i.e. the racemisation/epimerisation rate is not the same at sites with the same MAT, but located either in desert areas or in pluvial regions, because the effective insolation varies (Schmidt-Nielsen *et al.*, 1971).

Studies performed in the Negev desert, Israel, illustrate this (Goodfriend, 1987a, 1992). The MAT of the Negev (19.6 °C) suggests that similar and lower D-alle/L-Ile values measured in land snails should be expected in Madeira (19 °C) and Bermuda (21.7 °C), respectively (Table 13). However, the epimerisation ratios obtained in land snails from the Negev desert, with a MAT of 19.6 °C and low rainfall rates (178 mm yr^{-1}), are much higher (cf. Goodfriend, 1987a) than on the two islands (Table 11). In this case, D-alle/L-Ile values of 0.35 were observed in localities dated at ca. 10 ka BP, which approach those observed in the Canary Islands (D-alle/L-Ile = 0.40 for 23 ka BP). Furthermore, Goodfriend (1992) showed that the aspartic acid racemisation rate in gastropods from the Negev Desert was much higher than in land snails from Madeira.

This explains why the racemisation/epimerisation ratios of Madeira, Bermuda and Mallorca cannot be directly compared with Canary Island ratios. The location of the eastern Canary Archipelago (between 28 ° and 30 °N), close to the coast of Africa, is influenced by the cold Canary Current and Sahara desert winds, which reduce precipitation and cause high temperatures, equivalent to those recorded in the western Sahara Desert. In fact, the Negev desert and the Canary Archipelago belong to the same bioclimatic region (Mediterranean desertic-oceanic), while Bermuda is tropical pluvial, Mallorca is Mediterranean pluviseasonal-oceanic and Madeira is temperate hyperoceanic sub-Mediterranean (Table 13; Rivas-Martínez *et al.*, 2004).

Diverse studies corroborate the validity of our results. There is close correspondence with the dating of some volcanic rocks (mainly basalts) overlaid by aeolian deposits. The basaltic lava flows from Alegranza and Montaña Clara and some of the La Graciosa islets are linked to Upper Pleistocene and Holocene eruptions (Fig. 1; De La Nuez *et al.*, 1997; Ancochea *et al.*, 2004). Similarly, the volcanic rocks that crop out in the north of Fuerteventura and Lanzarote islands are Pleistocene. In fact, the basalts that crop out in the north of Fuerteventura (Fig. 1), which constitute the bottom of the Montaña de la Costilla (FMC) and Barranco de los Encantados (FBE) stratigraphic sections, were dated as younger than 51 ka BP (Pomel *et al.*, 1985) and older than 35 ka BP (Petit-Maire *et al.*, 1986). This means that aeolian deposits overlying these rocks are younger and, consequently, the ages obtained in our research are coherent.

Likewise, De La Nuez *et al.* (1997) dated the raised marine deposits from La Graciosa Islet (0 to +0.5 m above sea level), obtaining Holocene and Upper Pleistocene ages. Some of them are interbedded with the aeolian deposits, as in the Caleta del Sebo section. Limpet shells (*Patella* sp.) recovered from ancient marine deposits below bed GCS-1 provided a radiocarbon age of 28.7 ± 0.4 k ^{14}C yr BP (De La Nuez *et al.*, 1997).

Our results are also consistent with earlier studies of the aeolian/palaeosol formations (Table 14), especially those of Hillaire-Marcell *et al.* (1995) performed in the Teguise composite section, located in the north of Lanzarote, using ^{14}C, U/Th and amino acid racemisation. For D-alle/L-Ile ratios

Table 14 Comparison between the aminozones defined in this paper and global cold/dry episodes, Dune-formation episodes (ED) for the Chinijo Archipelago (De La Nuez *et al.*, 1997) and some stratigraphic sections previously studied in the eastern Canary Islands. The Rosa Negra section is also named Montaña de la Costilla (FMC). The locations of the sections are in Fig. 1. Much of these data come from radiocarbon dating of terrestrial gastropods with hard water effects requiring correction so they should be performed into calibrated ages (see Table 6 for comparison). One age was obtained through the radiocarbon analysis of an eggshell (es), which has to be transformed into a calibrated age. One age was obtained through thermoluminescence (TL)

Aminozones	Cold/dry episodes	Chinijo Archipelago	Jandía section	Corralejo section	Pozo Negro section	Rosa Negra section	Teguise section
AM-8 5.4 ± 1.1	4.0–4.2 ka						
	8.0–8.4 ka		7.93 ± 0.7 ^{14}C (3 & 4)	8.84 ± 0.7 ka (3 & 4)			
AM-7 11.0 ± 4.0	Y.D.	ED-V 11 ^{14}C ka (1)	9.8 ± 0.14 ^{14}C ka (2)		10–15 ka (TL) (2)		
AM-6 14.9 ± 3.6	H-1	ED-IV 18 ^{14}C ka (1)		15 ± 0.2 ka (2)			
AM-5 22.4 ± 4.5	H-2			23.22 ± 0.35 ka (3 & 4)	23.6 ± 0.55 ka (2)		
AM-4 29.4 ± 4.8	H-3	ED-III 30 ^{14}C ka (1)	28.95 ± 0.53 ^{14}C ka (3 & 4)-es			28.46 ± 0.63 ^{14}C ka (3 & 4)	Ps7:26.76 ± 0.23 ^{14}C ka (5)
			29.66 ± 0.66 ^{14}C ka (3 & 4)				
AM-3 37.8 ± 4.6	H-4		31.8 ± 0.15 ^{14}C ka (3 & 4)			32.5 ± 1.2 ^{14}C ka (3 & 4)	Ps6: 33.91 ± 0.38 ^{14}C ka (5)
			32.1 ± 1.11 ^{14}C ka (3 & 4)				
							Ps5: 34.2 ± 0.37 ^{14}C ka (5)
AM-2 42.5 ± 6.0		ED-II 38 ^{14}C ka (1)					Ps4: 37.42 ± 0.49 ^{14}C ka (5)
							Ps3: 38.73 ± 0.5 ^{14}C ka (5)
							Ps2: 38.27 ± 0.72 ^{14}C ka (5)
							Ps1: 40.76 ± 0.6 ^{14}C ka (5)
AM-1 48.6 ± 6.4	H-5	? ED-I MIS 3 (1)					

AM: aminozones; H: Heinrich Events; Y.D. Younger Dryas; ED: dune-formation episodes for Chinijo Archipelago; Ps: palaeosol; TL: thermoluminescence; es: eggshell. (1) de La Nuez *et al.* (1997); (2) Petit-Maire *et al.* (1986); (3) Damnati *et al.* (1996); (4) Meco *et al.* (1997); (5) Hillaire-Marcel *et al.* (1995).

of ca. 0.50 obtained (by IE-LC) in *Helicella* (Helicidae) land snails, the ages calculated are ca. 38 ka. In fact, the succession of aeolian deposits and palaeosols from this section correlate with some of the aminozones established in this paper. As the datings of the Teguise palaeosols are ^{14}C-ages and as a correction needs to be applied to transform them into calibrated years (see Table 6 for comparison), palaeosols 1 to 4 from this section can be included within Aminozone 2, palaeosols 5 and 6 can be grouped into Aminozone 3, and, finally, palaeosol 7 can be included in Aminozone 4.

Some of our aminozones might be recognised in other sections from Fuerteventura (Table 14), dated by Petit-Maire *et al.* (1986), Damnati *et al.* (1996) and Meco *et al.* (1997). Although many of these data come from the radiocarbon dating of terrestrial gastropods, with strong hard water effects requiring correction, especially in the youngest ones, and then transformation into calibrated ages, these dates coincide with the results obtained in this paper.

Amino acid geochronology of the Montaña de la Costilla section (Fuerteventura Island), also named the Rosa Negra section by other authors, corroborates the radiocarbon ages obtained by Meco *et al.* (1997), but not those obtained with optically stimulated luminescence (OSL) by Bouab and Lamothe (1997), using infrared stimulation of potassic feldspars (181 ± 27 ka, 183 ± 27 ka and 318 ± 45 ka). Probably the assumption that these sediments were zeroed during transport (Bouab and Lamothe, 1997) was not correct at all, as their ages were anomalously old. In fact, according to Pomel *et al.* (1985) and Petit-Maire *et al.* (1986), aeolian deposition started in this area not before 51 ka BP, but after 35 k ^{14}C yr BP.

Land snails from different horizons of the Mala section (Lanzarote Island) were U/Th dated at ca. 95, 138, 235 and >350 ka (Shimmield, in Meco *et al.*, 1997), in clear variance from our data. Owing to the consistency observed between the D/L ratios measured in gastropods from the Mala section and those from other localities, the bad fit between U/Th ages and stratigraphy (cf. Meco *et al.*, 1997) and the problems regarding reliability of U/Th dating of molluscs (Kaufman *et al.*, 1971, 1996), especially from palaeosols, it seems that the earlier ages were wrong and that the Mala section timespan runs between ca. 40 and 29 ka BP.

Our data are in agreement with De La Nuez *et al.* (1997), who defined five dune-formation episodes for the Chinijo Archipelago (ED-I to ED-V). The aeolian deposits of the first episode (ED-I) are located above basaltic flows and sandstones from MIS 5 and, according to De La Nuez *et al.* (1997), could belong to MIS 3. The remaining episodes (ED-II to ED-V) were dated at ca. 37 k ^{14}C yr BP, 30 k ^{14}C yr BP, 15 k ^{14}C yr BP and 11 k ^{14}C yr BP respectively. All these dune-formation episodes correlate with the aminozones defined here (Table 14).

Since aeolian deposits accumulated during arid phases and palaeosols developed during humid periods (Petit-Maire *et al.*, 1986, 1987; Rognon and Coudé-Gaussen, 1988, 1996a; Damnati *et al.*, 1996; Damnati, 1997; De La Nuez *et al.*, 1997), close correspondence is found between the dune formation episodes of the eastern Canary Islands and the climate variations across North Africa. At least five alternations of dry/humid episodes have been inferred from the amino acid racemisation ages obtained in gastropods from the easternmost islands and islets of the Canary Archipelago preceding the Last Glacial Maximum (23–18 ka BP). Similarly, arid phases, followed by humid periods with abrupt transitions, occurred in North Africa from 50 to 23 ka BP (Gasse (2000) and references therein), which, in their opinion, cannot be directly attributed to orbital forcing.

After the Last Glacial Maximum (LGM), two significant arid–humid transitions have been documented at ca. 15 ka and 11 ka BP across Africa (Street-Perrott and Perrott, 1990; Gasse *et al.*, 1990; Talbot and Johannessen, 1992; Gasse and Van Campo, 1994). During the Holocene, major dry spells took place around 8.4–8 and 4.2–4 ka BP (Talbot *et al.*, 1984; Gasse *et al.*, 1990; Street-Perrott *et al.*, 1990; Lamb *et al.*, 1995; Holmes *et al.*, 1999). Three of these phases of aridification (ca. 15, 11 and 4 ka BP) coincide with the age of the dune-formation episodes documented by Aminozones 6, 7 and 8 in the eastern Canary Islands and Islets. However, in our studies we did not find the ca. 8 ka dune-formation episode, as recognised elsewhere in the Canary Archipelago (Petit-Maire *et al.*, 1987; Damnati *et al.*, 1996).

Studies of aeolian deposits from the Sahara (Swezey, 2001) show similar results, which coincide with atmospheric and oceanic changes. Moreover, our results can be compared with the record of Lake Bosumtwi (Ghana), which lies in the path of the seasonal migration of the intertropical convergence zone (ITCZ) and, therefore, is ideally located for the study of monsoon variability in West Africa (cf. Peck *et al.*, 2004). Aminozones 5, 6 and 7 correlate with the episodes of high concentrations of high-coercivity iron sulfide magnetic minerals dated at ca. 12.5, 17.3 and 22.6 ka BP of Lake Bosumtwi, which reflect episodes of increased aeolian dust transport from the Sahel. According to Peck *et al.* (2004), periods of increased regional aridity and greater dust flux out of the Sahel source regions were caused by a southward movement of the ITCZ and weakened monsoon strength, whereas humid periods and, consequently, lower dust fluxes were linked to stronger monsoon activity when the ITCZ moved northwards. Similarly, the dry events which produced the accumulation of Canary Islands aeolian deposits belonging to Aminozones 1 and 2 correlate with the transitions between 12 to 11 and 9 to 8 Dansgaard/Oeschger Events, interpreted from the oxygen isotope ratios of calcite in a stalagmite found on Socotra Island (Yemen, western Indian Ocean) (Burns *et al.*, 2003). Clearly, the stalagmite from Socotra is a continuous record, whereas the Canaries dunes and palaeosols are discontinuous. Thus, similar patterns are observed in the behaviour of palaeomonsoons in West Africa and in East Africa–India (cf. Gasse, 2000; Moreno *et al.*, 2001; Burns *et al.*, 2003). This synchroneity suggests that a global forcing mechanism caused changes in African and Indian monsoon activity and controlled the arid/humid changes documented in the Canary Islands and North Africa, at least during the last 50 ka BP. Therefore, the rapid dryings of North Africa cannot be explained only in terms of internal, mainly regional, vegetation–atmosphere feedbacks in the climate system, because the timing of these events depends on the state of the global climate system (Gasse, 2000). In fact, according to Burns *et al.* (2003), there is a strong connection between the climate of the tropical East Africa region and the Indian Ocean (monsoon activity) and temperature variations in the North Atlantic region.

Agreeing with conclusions of Peck *et al.* (2004), Moreno *et al.* (2001) showed that insolation changes during the Pleistocene played an important role in modulating dust supply within the Canary Basin, with arid–humid scenarios attributed to changes in the strength of palaeomonsoon activity (Fig. 9). During 'arid' episodes, palaeomonsoon winds were enhanced and the trade winds (flowing in an easterly direction along the entire coast) were intensified, causing the transport of aeolian materials from a northwest African source, while the Saharan Air Layer became less intense. On the contrary, during 'humid' episodes, the palaeomonsoons may have become weaker, which would have caused a major influence of the Saharan winds on the Canary Archipelago, associated with the north-turning of part of the Saharan Air Layer (Raltmeyer *et al.*, 1999). During these episodes, aeolian accumulation was

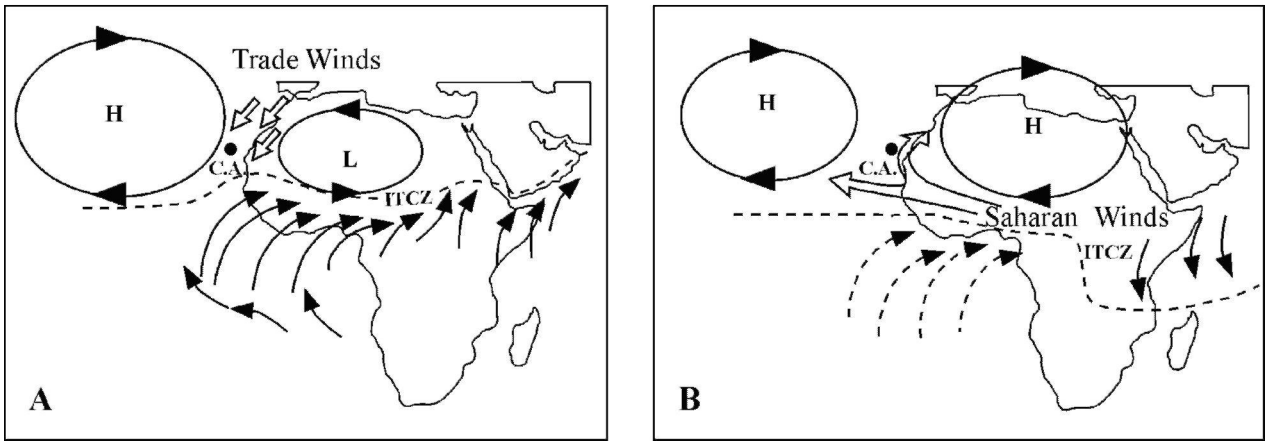

Figure 9 Inferred climate scenarios (modified from Nicholson (1996) and Moreno *et al.*, 2001) for the (A) humid episodes and (B) arid episodes in Africa. Black arrows represent the monsoon winds; weaker winds are plotted by dashed arrows. During 'humid' episodes, monsoon winds were enhanced and trade winds, which turn to be more easterly directions on the entire coast, were intensified which resulted in the transport of materials from a northwest African source, while the Saharan Air Layer becomes less intense. On the other hand, during 'arid' episodes, the monsoons became weaker producing a major influence of the Saharan winds in the Canary Archipelago by a north-turning part of the Saharan Air Layer. The location of the Canary Archipelago (C.A.) is represented by a black dot

produced by west-to-east or southwest-to-northeast winds that carried biodetrital sands from emerged continental shelves onto the land (Rognon and Coudé-Gaussen, 1988, 1996b). Typically, arid periods coincided with cold events, while increasing moisture (rainfall) coexisted with warm phases (Gasse, 2000; Peck *et al.*, 2004).

The 250 ka long marine records studied by Moreno *et al.* (2001) suggest that insolation changes related to eccentricity and precession are the main forcing mechanisms for this region. However, there could be other mechanisms to explain the shorter cycles of dune/palaeosol formations. The monsoon reactivations led to a moderate moisture (rainfall) rise. These events have already been associated with the abrupt temperature changes in Greenland ice cores at the onset of the Bölling and Preboreal periods, and with the switch to the modern mode of North Atlantic deep-water production (Street-Perrott and Perrott, 1990; Gasse and Van Campo, 1994; Gasse, 2000).

The causes of the abrupt Holocene events are not known (Gasse, 2002). Some authors suggested a decrease in North Atlantic thermohaline circulation around 8.2 ka BP caused by an increase in freshwater flux to the North Atlantic (Alley *et al.*, 1997), whereas Gasse and Van Campo (1994) noted that the weak monsoon episodes around 8 and 4 ka BP roughly coincide with decreases in North Atlantic sea surface temperature and surface salinity. The antiphase between rainfall changes in Equatorial West Africa and in the Amazon may reflect changes either in Walker circulation and ENSO phenomena or in Hadley circulation, e.g. a strengthening of the northern trade winds at ca. 4 ka BP bringing dry weather. In any case, the worldwide impact of these events implies that rapid changes in the water cycle in Africa are the expression of global climate reorganisation (Gasse, 2002).

According to the aminostratigraphic and aminochronological data reported in this paper, the events of aeolian deposition before and after the LGM took place with a cyclicity lasting between five and seven millennia. It is possible that the deposition of dunes and palaeosol formation could be related to variations in solar radiation, which may have forced climate changes (Eddy, 1982; Rasporov *et al.*, 1998).

In our case, the aeolian-palaeosol cycles, with a periodicity of between five and seven millennia, could be interpreted as being the expression of multiples of the solar activity cycle of about 2.4 ka (cf. Hood and Jirikowic, 1991), which, according to Charvátová (2000), is probably linked to solar inertial motion. In the view of Dergachev and Chistiakov (1998), this 2.4 ka solar cycle includes three parts roughly equal in duration: a phase of high activity (climatic optimum), a phase of depression (cold conditions) and a phase of moderate activity (temperate climate).

Conclusions

The first aminochronological and aminostratigraphical results of Quaternary aeolian/palaeosol deposits from the eastern islands (Fuerteventura and Lanzarote) and islets (La Graciosa, Montaña Clara and Alegranza) of the Canary Archipelago came from analysis of *Theba* shells. The study focused on four amino acids, isoleucine, aspartic acid, phenylalanine and glutamic acid, because of the high correlation coefficients between their D/L ratios. The age calculation algorithms of these amino acids were also established and the following were chosen: the first-order-reversible kinetic (FOK) transformation of the D/L ratios versus the square root of time for aspartic acid, the untransformed D/L ratios (APK) versus the square root of time for phenylalanine and glutamic acid, and the untransformed D/L ratios (APK) versus time for isoleucine. With the aid of these algorithms, age estimates of the aeolian deposits from the islands were calculated.

Eight aminozones, representing episodes of dune formation, were established: Aminozone 1 (48.6 ± 6.4 ka BP), 2 (42.5 ± 6.0 ka BP), 3 (37.8 ± 4.6 ka BP), 4 (29.4 ± 4.8 ka BP), 5 (22.4 ± 4.5 ka BP), 6 (14.9 ± 3.6 ka BP), 7 (11.0 ± 4.0 ka BP) and 8 (5.4 ± 1.1 ka BP).

These and previous results show that aeolian/palaeosol deposits accumulated between MIS 1 and 3 during arid phases, with a recurrence period of 5–7 ka, which stopped when conditions produced higher effective environmental moisture and soil formation.

Synchroneity with the palaeoclimate in Africa (Fig. 9) was observed, suggesting that a global forcing mechanism (not related to orbital forcing) controlled the climate changes in the Canary Islands and North Africa at least during the last 50 ka BP. This could be linked to palaeomonsoon activity,

which caused predominance of trade winds during humid phases and of Saharan winds during arid episodes.

These aeolian cycles with a periodicity of five to seven millennia might be interpreted as being the expression of multiples of the ~2.4 ka solar cycle in continental sediments.

Acknowledgements Funding was obtained through the projects PI2001/044 from Consejería de Educación, Cultura y Deporte del Gobierno de Canarias, and BOS2003/00374 from the Ministerio de Ciencia y Tecnología. We thank to Dr T. Roca (La Laguna University) and Professor E. Chacón (E.T.S.I. Minas) who helped in the comments about discussion. We are indebted to Dr V. Meyer (Bern University) who helped in the setting up of our laboratory. The Biomolecular Stratigraphy Laboratory has been partially funded by ENRESA. We thank Professor Paul Hearty and an anonymous reviewer for their helpful comments.

References

Alley R, Mayewski P, Sowers T, Stuiver M, Taylor K, Clark P. 1997. Holocene climatic instability: a prominent, widespread event 8200 yr ago. *Geology* **25**: 483–486.

Alonso-Zarza AM, Silva PG. 2002. Quaternary laminar calcretes with bee nests: evidences of small-scale climatic fluctuations, Eastern Canary Islands, Spain. *Palaeogeography Palaeoclimatology Palaeoecology* **178**: 119–135.

Ancochea E, Brändle JL, Cubas CR, Hernán F, Huertas MJ. 1996. Volcanic complexes in the eastern ridge of the Canary Islands: the Miocene activity of the island of Fuerteventura. *Journal of Volcanology and Geothermal Research* **70**: 183–204.

Ancochea E, Barrera JL, Bellido F, Benito R, Brändle JL, Cebriá JM, Coello J, Cubas CR, De la Nuez J, Doblas M, Gómez JA, Hernán F, Herrera R, Huertas MJ, López Ruiz J, Martí J, Muñoz M, Sagredo J. 2004. Canarias y el vulcanismo neógeno Peninsular. In *Geología de España*, Vera JA (ed). Sociedad Geológica de España-Instituto Geológico y Minero de España: Madrid; 635–682.

Bada JL, Schroeder RA. 1972. Racemization of isoleucine in calcareous marine sediments: kinetics and mechanism. *Earth and Planetary Science Letters* **15**: 1–11.

Bouab N, Lamothe M. 1997. Geochronological framework for the Quaternary paleoclimatic record of the Rosa Negra section (Fuerteventura-Canary Islands, Spain). In *Climates of the Past. Fuerteventura and Lanzarote*, Meco J, Petit-Maire N (eds). International Union of Geological Sciences, UNESCO: Las Palmas de Gran Canaria; 37–42.

Boye P, Hutterer R, López-Martínez N, Michaux J. 1992. A reconstruction of the lava mouse (Malpaisomis insularis), an extinct rodent of the Canary Islands. *Zeitschrift fur Säugetierkunde* **57**: 29–38.

Brooke BP, Murray-Wallace CV, Woodroffe CD, Heijns H. 2003. Quaternary aminostratigraphy of eolianite on Lord Howe Island, Southwest Pacific Ocean. *Quaternary Science Reviews* **22**: 387–406.

Burns SJ, Fleitman D, Matter A, Kramers J, Al-Subbary AA. 2003. Indian Ocean climate and an absolute chronology over Dansgaard/Oeschger Events 9 to 13. *Science* **301**: 1365–1367.

Carracedo JC, Rodríguez Badiola E. 1993. Evolución geológica y magmática de la isla de Lanzarote (Islas Canarias). *Revista de la Academia Canaria de la Ciencia* **4**: 25–58.

Castillo C, López M, Martín M, Rando C. 1996. La paleontología de vertebrados en Canarias. *Revista Española de Paleontología*, special issue: 237–247.

Castillo C, Martín-González E, Yanes Y, Ibáñez M, De la Nuez J, Alonso MR, Quesada ML. 2002. Estudio preliminar de los depósitos dunares de los Islotes del Norte de Lanzarote. Implicaciones paleoambientales. *Geogaceta* **32**: 79–82.

Charvátová I. 2000. Can origin of the 2400-year cycle of solar activity be caused by solar inertial motion? *Annales Geophysicae* **18**: 399–405.

Coello J, Cantagrel JM, Hernán F, Fúster JM, Ibarrola E, Ancochea E, Casquet C, Jamond C, Díaz de Terán JR, Cendrero A. 1992. Evolution of the eastern volcanic ridge of the Canary Islands based on new K-Ar data. *Journal of Volcanology and Geothermal Research* **53**: 251–274.

Csapò J, Csapó-Kiss Z, Csapó JJR, 1998. Use of amino acids for age determination in archaeometry. *Trends in Analytical Chemistry* **17**: 140–148.

Damnati B. 1997. Mineralogical and sedimentological characterization of Quaternary eolian formations and paleosoils in Fuerteventura and Lanzarote (Canary Islands, Spain). In *Climates of the Past: Lanzarote and Fuerteventura*, Meco J, Petit-Maire N (eds). International Union of Geological Sciences, UNESCO: Las Palmas de Gran Canaria; 71–77.

Damnati B, Petit-Maire N, Fontugne M, Meco J, Williamson D. 1996. Quaternary palaeoclimates in the eastern Canary Islands. *Quaternary International* **31**: 37–46.

De La Nuez J, Quesada ML, Alonso JJ, Castillo C, Martín E. 1997. Edad de los Islotes en función de los datos paleontológicos. In *Los Volcanes de los Islotes al Norte de Lanzarote*, De La Nuez J, Quesada ML, Alonso JJ (eds). Fundación César Manrique: Lanzarote; 73–81.

Dergachev VA, Chistiakov VF. 1998. Effect of the approximately 2400-year solar climatic cycle on the lives of peoples. *Biofizika* **43**: 940–944.

Eddy JA. 1982. The solar constant and surface temperature. In *Interpretation of Climate and Photochemical Models, Ozone and Temperature Measurements*, Peck RA, Hummel JR (eds). American Institute of Physics: New York.

Edwards N, Meco J. 2000. Morphology and palaeoenvironment of brood cells of Quaternary ground-nesting solitary bees (Hymenoptera, Apidae) from Fuerteventura, Canary Islands, Spain. *Proceedings of the Geologists Association* **111**: 173–183.

Ellis WN, Ellis-Adam AC. 1993. Fossil brood cells of solitary bees on Fuerteventura and Lanzarote, Canary Islands (Hymenoptera: Apoidea). *Entomologische Berichten* **53**: 161–173.

Ellis GL, Goodfriend GA, Abbott JT, Hare PE, Von Endt DW. 1996. Assessment of integrity and geochronology of archaeological sites using amino acid racemization in land snail shells: examples from central Texas. *Geoarcheology: An International Journal* **11**: 189–213.

Fúster JM, Fernández Santín S, Sagredo J. 1968. *Geología y Volcanología de las Islas Canarias. Lanzarote.* Instituto Lucas Mallada, C.S.I.C.: Madrid.

Gasse F. 2000. Hydrological changes in the African tropics since the Last Glacial Maximum. *Quaternary Science Reviews* **19**: 189–211.

Gasse F. 2002. Diatom-inferred salinity and carbonate oxygen isotopes in Holocene waterbodies of the western Sahara and Sahel (Africa). *Quaternary Science Reviews* **21**: 737–767.

Gasse F, Van Campo E. 1994. Abrupt post-glacial climate events in West Asia and North Africa monsoon domains. *Earth and Planetary Science Letters* **126**: 435–456.

Gasse F, Téhet R, Durand A, Gibert E, Fontes JC. 1990. The arid–humid transition in the Sahara and the Sahel during the last deglaciation. *Nature* **346**: 141–156.

Genise JF, Edwards N. 2003. Ichnotaxonomy, origin, and paleoenvironment of Quaternary insect cells from Fuerteventura, Canary Islands, Spain. *Journal of the Kansas Entomological Society* **76**: 320–327.

Gittenberger E, Ripken TEJ. 1987. The genus Theba (Mollusca: Gastropoda: Helicidae). Systematics and distribution. *Zoologische Verhandelingen* **241**: 1–62.

Gittenberger E, Ripken TEJ, Bueno ML. 1992. The forgotten Theba species (Gastropoda, Pulmonata, Helicidae). *Proceedings of the 10th Malacological Congress*. Gittenberger and Goud: Edinburgh; 145–151.

Goodfriend GA. 1987a. Chronostratigraphic studies of sediments in the Negev Desert, using amino acid epimerization analysis of land snails shells. *Quaternary Research* **28**: 374–392.

Goodfriend GA. 1987b. Radiocarbon age anomalies in shell carbonate of land snails from semi-arid areas. *Radiocarbon* **29**: 159–167.

Goodfriend GA. 1991. Patterns of racemization and epimerisation of aminoacids in land snails shells over the course of the Holocene. *Geochimica et Cosmochimica Acta* **55**: 293–302.

Goodfriend GA. 1992. Rapid racemization of aspartic acid in mollusc shells and potential for dating over recent centuries. *Nature* **357**: 399–401.

Goodfriend GA, Hood DG. 1983. Carbon isotope analysis of land snail shells: implications for carbon sources and radiocarbon dating. *Radiocarbon* **25**: 810–830.

Goodfriend GA, Meyer RR. 1991. A comparative study of the kinetics of amino acid racemization/epimerization in fossil and modern mollusk shells. *Geochimica et Cosmochimica Acta* **55**: 3355–3367.

Goodfriend GA, Mitterer RM. 1988. Late Quaternary land snails from the north coast of Jamaica: local extinctions and climatic change. *Palaeogeography Palaeoclimatology Palaeoecology* **63**: 293–312.

Goodfriend GA, Stipp DG. 1983. Limestone and the problem of radiocarbon dating of land-snail shell carbonate. *Geology* **11**: 575–577.

Goodfriend GA, Hare PE, Druffel ERM. 1992. Aspartic acid racemization and protein diagenesis in corals over the last 350 years. *Geochimica et Cosmochimica Acta* **56**: 3847–3850.

Goodfriend GA, Kashgarian M, Harasewych MG. 1995. Use of aspartic acid racemization and post-bomb ^{14}C to reconstruct growth rate and longevity of the deep-water slit shell Entemnotrochus adansonianus. *Geochimica et Cosmochimica Acta* **59**: 1125–1129.

Goodfriend GA, Brigham-Grette J, Miller GH. 1996. Enhanced age resolution of the marine Quaternary record in the Arctic using aspartic acid racemization dating of bivalve shells. *Quaternary Research* **45**: 176–187.

Goodfriend GA, Ellis GL, Toolin LG. 1999. Radiocarbon age anomalies in land snail shells from Texas: ontogenic, individual, and geographic patterns of variation. *Radiocarbon* **41**: 149–156.

Hare PE, Mitterer RM. 1968. Laboratory stimulation of amino acid diagenesis in fossils. *Carnegie Institution of Washington Yearbook* **67**: 205–208.

Hearty PJ. 1987. New data on the Pleistocene of Mallorca. *Quaternary Science Reviews* **6**: 245–257.

Hearty PJ. 2003. Stratigraphy and timing of eolianite deposition on Rottnest Island, Western Australia. *Quaternary Research* **60**: 211–222.

Hearty PJ, Vacher HL, Mitterer RM. 1992. Aminostratigraphy and ages of Pleistocene limestones of Bermuda. *Geological Society of American Bulletin* **104**: 471–480.

Hearty PJ, Kindler P, Cheng H, Edwards RL. 1999. A +20 m middle Pleistocene sea-level highstand (Bermuda and the Bahamas) due to partial collapse of Antarctic ice. *Geology* **27**: 375–378.

Hearty PJ, Kaufman DS, Olson SL, James HF. 2000. Stratigraphy and whole-rock amino acid geochronology of key Holocene and Last Interglacial carbonate deposits in the Hawaiian Islands. *Pacific Science* **54**: 423–442.

Hearty PJ, Miller GH, Stearns CE, Szabo BJ. 1986. Aminostratigraphy of Quaternary shorelines in the Mediterranean Basin. *Geological Society of America Bulletin* **97**: 850–858.

Hillaire-Marcel C, Ghaler M, Gariépy C, Zazo C, Hoyos M, Goy JJ. 1995. U-series dating by the TIMS technique of land snails from paleosols in the Canary Islands. *Quaternary Research* **44**: 276–282.

Holmes JA, Street-Perrott FA, Perrott RA, Stokes S, Waller MP, Huang Y, Eglington G, Ivanovich M. 1999. Environmental change, lake and groundwater in the Sahel of Northern Nigeria. Part 2. Holocene landscape evolution of the Manga grasslands. Evidence from palaeolimnology and dune chronology. *Journal of the Geological Society London* **155**: 357–358.

Hood LL, Jirikowic JL. 1991. A probable 2400 year solar quasi-cycle in atmospheric $\delta^{14}C$. *Holocene* **12**: 98–105.

Kaufman A, Broecker WS, Ku TL, Thurber DL. 1971. The status of U-series methods of mollusk dating. *Geochimica et Cosmochimica Acta* **35**: 1115–1183.

Kaufman A, Ghaleb B, Wehmiller JF, Hillaire-Marcel C. 1996. Uranium concentration and isotope ratio profiles within Mercenaria shells: geochronological implications. *Geochimica et Cosmochimica Acta* **60**: 3735–3746.

Kaufman DS. 2000. Amino acid racemization in ostracodes. In *Perspectives in Amino Acid and Protein Geochemistry*, Goodfriend G, Collins M, Fogel M, Macko S, Wehmiller J (eds). Oxford University Press: New York; 145–160.

Kaufman DS. 2003. Amino acid paleothermometry of Quaternary ostracodes from the Bonneville Basin, Utah. *Quaternary Science Reviews* **22**: 899–914.

Kindler P, Hearty PJ. 1995. Pre-Sangamonian eolianites in the Bahamas? New evidence from Eleuthera Island. *Marine Geology* **127**: 73–86.

Kriausakul N, Mitterer RM. 1980. Comparison of isoleucine epimerization in a model dipeptide and fossil protein. *Geochimica et Cosmochimica Acta* **44**: 753–758.

Lamb HF, Gasse F, Ben Kaddour A, El Hamouti N, Van der Kaars S, Perkins WT, Pearce NJ, Roberts CN. 1995. Relation between century-scale Holocene arid intervals in tropical and temperate zones. *Nature* **373**: 134–137.

Levin I, Hesshaimer V. 2000. Radiocarbon-a unique tracer of global carbon cycle dynamics. *Radiocarbon* **43**: 69–80.

Manley WF, Miller GH, Czywczynski J. 2000. Kinetics of aspartic acid racemization in Mya and Hiatella: modelling age and paleotemperature of high-latitude Quaternary molluscs. In *Perspectives in Amino Acid and Protein Geochemistry*, Goodfriend GA, Collins MJ, Fogel ML, Macko SA, Wehmiller JF (eds). Oxford University Press: New York; 202–218.

Masters PM, Bada JL. 1977. Racemization of fossil molluscs from the indian middens and interglacial terraces in Southern California. *Earth and Planetary Science Letters* **37**: 173–183.

Meco J, Petit-Maire N, Fontugne M, Shimmield G, Ramos AJ. 1997. The Quaternary deposits in Lanzarote and Fuerteventura (Eastern Canary Islands, Spain): an overview. In *Climates of the Past: Fuerteventura and Lanzarote*, Meco J, Petit-Maire N (eds). International Union of Geological Sciences, UNESCO: Las Palmas de Gran Canaria; 123–136.

Meyer VR. 1992. Amino acid racemization: a tool for fossil dating. Understand the kinetics of racemization, measure the D/L ratio, and you have an estimate of the age. *American Chemical Society* **July**: 412–417.

Michaux J, Hutterer R, Lopez-Martínez N. 1991. New fossil fauna from Fuerteventura, Canary Islands: evidence for a Pleistocene age of endemic rodents and shrews. *Comptes Rendus de l'Académie des Sciences* **312**: 801–806.

Miller GH, Brigham-Grette J. 1989. Amino acid geochronology: resolution and precision in carbonate fossils. In *Applied Aspects of Quaternary Geochronology*, Rutter N, Brigham-Grette J, Catto N (eds). *Quaternary International* **1**: 111–128.

Miller GH, Wendorf F, Ernst R, Schild R, Close AE, Friedman I, Schwarcz HP. 1991. Dating lacustrine episodes in the eastern Sahara by the epimerization of isoleucine in ostrich eggshells. *Palaeogeography Palaeoclimatology Palaeoecology* **84**: 175–189.

Miller GH, Beaumont PB, Jull AJT, Johnson B. 1992. Pleistocene geochronology and paleothermometry from protein diagenesis in ostrich eggshells—implications for the evolution of modern humans. *Philosophical Transactions of the Royal Society of London Series B—Biological Sciences* **337**: 149–157.

Mitterer RM. 1975. Ages and diagenetic temperatures of Pleistocene deposits of Florida based on isoleucine epimerization in *Mercenaria*. *Earth and Planetary Science Letters* **28**: 275–282.

Mitterer RM, Kriasakul N. 1989. Calculation of amino acid racemization ages based on apparent parabolic kinetics. *Quaternary Science Reviews* **8**: 353–357.

Moreno A, Targarona J, Hendericks J, Canals M, Freudenthal T, Meggers H. 2001. Orbital forcing of dust suply to the north Canary Basin over the last 250 kyr. *Quaternary Science Reviews* **20**: 1327–1339.

Murray-Wallace CV. 1995. Aminostratigraphy of quaternary coastal sequences in southern Australia an overview. *Quaternary International* **26**: 69–86.

Murray-Wallace CV, Goede A. 1995. Aminostratigraphy and electron spin resonance dating of Quaternary coastal neotectonism in Tasmania and the Bass Strait islands. *Australian Journal of Earth Sciences* **42**: 51–67.

Murray-Wallace CV, Kimber RWL. 1993. Further evidence for apparent 'parabolic' racemization kinetics in Quaternary molluscs. *Australian Journal of Earth Sciences* **40**: 313–317.

Murray-Wallace CV, Brooke BP, Cann JH, Belperio AP, Bourman RP. 2001. Whole rock aminostratigraphy of the Coorong Coastal Plain,

South Australia: towards a 1 million year record of sea-level highstands. *Journal of the Geological Society of London* **158**: 111–124.

Nicholson SE. 1996. A review of climate dynamics and climate variability in Eastern Africa. In *The Limnology, Climatology and Paleoclimatology of the East African Lakes*, Johnson TC, Odada EO (eds). Gordon & Breach: Amsterdam; 25–56.

Ortiz JE, Torres T, Llamas FJ. 2002. Cross-calibration of the racemization rates of leucine and phenylalanine and epimerization rates of isoleucine between ostracodes and gastropods over the Pleistocene in southern Spain. *Organic Geochemistry* **33**: 691–699.

Ortiz JE, Torres T, Julià R, Delgado A, Llamas FJ, Soler V, Delgado J. 2004. Numerical dating algorithms of amino acid racemization ratios from continental ostracodes. Application to the Guadix-Baza Basin (southern Spain). *Quaternary Science Reviews* **23**: 717–730.

Ortiz JE, Torres T, Julià R, Llamas JF. 2005. Algoritmos de cálculo de edad a partir de relaciones de racemización/epimerización de aminoácidos en pelecípodos marinos del litoral mediterráneo español. *Revista de la Sociedad Geológica de España* **17**: 217–227.

Peck JA, Green RR, Shanahan T, King JW, Overpeck JT, Scholz CA. 2004. A magnetic mineral record of Late Quaternary tropical climate variability from Lake Bosumtwi, Ghana. *Palaeogeography, Palaeoclimatology, Palaeoecology* **215**: 37–57.

Petit-Maire N, Delibrias G, Pomel S, Rosso JC. 1986. Paleoclimatologie des Canaries orientales (Fuerteventura). *Comptes Rendus de l'Académie des Sciences Paris* **303**: 1241–1246.

Petit-Maire N, Rosso JC, Delibrias G, Meco J, Pomel S. 1987. Paléoclimats de l'île de Fuerteventura (Archipel Canarien). *Palaeoecology of Africa and the Surrounding Islands* **18**: 351–356.

Pomel RS, Miallier D, Fain J, Sanzelle S. 1985. Datation d'un sol brun-rouge calcifère par una coulée d'âge Würm ancien (51 000 ans) à Fuerteventura (Iles Canaries). *Méditerranée* **4**: 59–68.

Quesada ML, De La Nuez J, Alonso JJ. 1992. Edificios hidromagmáticos en las Isletas del Norte de Lanzarote. *Actas III Congreso Geológico de España y VIII Congreso Latinoamericano de Geología. Salamanca* vol. 1. Civis and Flores: Salamanca; 473–476.

Raltmeyer V, Fischer G, Wefer G. 1999. Lithogenic particle fluxes and grain size distributions in the deep ocean off northwest Africa: implications for seasonal changes of Aeolian dust input and downward transport. *Deep-Sea Research I* **46**: 1289–1337.

Raspopov OM, Shumilov OI, Kasatkina EA. 1998. Cosmic rays as the main factor affecting solar variability on climatic and atmospheric parameters. *Biofizika* **43**: 902–908.

Rivas-Martínez S, Rivas y Sáenz S. 2005. Worldwide Bioclimatic Classification System. www.globalbioclimatics.org [15 April 2005].

Rivas-Martínez S, Penas A, Díaz TE. 2004. Bioclimatic Map of Europe, Thermoclimatic Belts. www.globalbioclimatics.org [15 July 2004].

Rognon P, Coudé-Gaussen G. 1988. Origine eolienne de certains encroutements calcaires sur l'ile de fuerteventura (Canaires orientales). *Geoderma* **42**: 217–293.

Rognon P, Coudé-Gaussen G. 1996a. Changements dans les circulations atmosphérique et océanique à la latitude des Canaries et du Maroc entre les stades isotopiques 2 et 1. *Quaternaire* **7**: 197–206.

Rognon P, Coudé-Gaussen G. 1996b. Paleoclimates off northwest Africa (28°–35°N) about 18 000 yr B.P. based on continental eolian deposits. *Quaternary International* **46**: 118–126.

Schmidt-Nielsen K, Taylor CP, Schkolnik A. 1971. Desert snails: problems of heat, water and food. *Journal of Experimental Biology* **55**: 385–398.

Street-Perrott FA, Perrott RA. 1990. Abrupt climate fluctuations in the tropics: the influence of Atlantic Ocean Circulation. *Nature* **343**: 607–611.

Street-Perrott FA, Mitchell JFB, Marchand DS, Brunner JS. 1990. Milankovitch and albedo forcing on the tropical monsoons: a comparison of geological evidence and numerical simulations for 9000 yr BP. *Transactions of the Royal Society of Edinburgh—Earth Sciences* **81**: 407–427.

Stuiver M, Reimer PJ. 1993. Extended ^{14}C database and revised CALIB radiocarbon calibration program. *Radiocarbon* **35**: 215–230.

Stuiver M, Reimer PJ, Bard E, Beck JW, Burr GS, Hughen KA, Kromer B, McCormac FG, van der Plicht J, Spurk M. 1998. INTCAL98 Radiocarbon age calibration 24 000–0 cal BP. *Radiocarbon* **40**: 1041–1083.

Swezey C. 2001. Eolian sediment responses to late Quaternary climate changes: temporal and spatial patterns in the Sahara. *Palaeogeography, Palaeoclimatology, Palaeoecology* **167**: 119–155.

Talbot MR, Johannessen T. 1992. A high resolution palaeoclimatic record of the last 27 500 years in tropical West Africa from the carbon and nitrogen isotopic composition of lacustrine organic matter. *Earth and Planetary Science Letters* **110**: 23–37.

Talbot MR, Livingstone DA, Palmer DG, Maley J, Melack JM, Delibrias G, Gulliksen J. 1984. Preliminary results from sediments core from lake Bosumtwi, Ghana. *Palaeoecology of Africa* **16**: 173–192.

Torres T, Llamas J, Canoira L, García-Alonso P, García-Cortés A, Mansilla H. 1997. Amino acid chronology of the Lower Pleistocene deposits of Venta Micena (Orce, Granada, Andalusia, Spain). *Organic Geochemistry* **26**: 85–97.

Vacher HL, Hearty PJ, Rowe MP. 1995. Stratigraphy of Bermuda: nomenclature, concepts, and status of multiple systems of classification. In *Terrestrial and Shallow Marine Geology of the Bahamas and Bermuda*, Curran HA, White B (eds). *Geological Society of America* Special paper no. 300: 271–294.

Wehmiller JF. 1984. Interlaboratory comparison of amino acid enantiomeric ratios in fossil Pleistocene mollusk. *Quaternary Research* **22**: 109–120.

Wehmiller JF, Hare PE. 1971. Racemization of amino acids in marine sediments. *Science* **173**: 907–911.

Weninger B, Jöris O, Danzeglocke U. 2004. http://www.calpal-online.de/ [7 July 2004].

Yanes Y, Castillo C, Alonso MR, Ibáñez M, De La Nuez J, Quesada ML, Martín-González E, La Roche F, Liché D, Armas RF. 2004. Gasterópodos terrestres Cuaternarios del Archipiélago Chinijo, Islas Canarias. *Vieraea* **32**: 123–134.